This article has been accepted for publication in a future issue of this journal, but has not been fully edited. Content may change prior to final publication. Citation information: DOI 10.1109/TAES.2018.2831118, IEEE Transactions on Aerospace and Electronic Systems

Source localization based on acoustic single direction measurements

Joel Reis, Pedro Batista, *Member, IEEE,* Paulo Oliveira, *Senior Member, IEEE,* and Carlos Silvestre, *Member, IEEE*

***Abstract*—This paper presents a novel filtering technique to estimate the position of a moving target based on discrete-time direction and velocity measurements. The velocity is assumed to be corrupted by an unknown constant bias, which is explicitly estimated in the process. A nonlinear system is first designed, describing the dynamics and observations associated to the target, followed then by a state augmentation that yields an equivalent linear time-varying system. An observability analysis for the latter is conducted based on necessary and sufficient conditions that are related to the target's motion. The final estimation solution resorts to a Kalman Filter with globally exponentially stable error dynamics. Its performance is assessed via realistic numerical simulations, including Monte Carlo runs and a comparison with both the standard Extended Kalman Filter and the Bayesian Cramér-Rao bound. A set of experimental results achieved within the scope of a realistic underwater mission scenario is also presented that allows to further assess the proposed technique.**

***Index Terms*—Source Localization, Global Exponential Stability, Uniform Complete Observability, Kalman Filter, Bayesian Cramér-Rao bound**

I. INTRODUCTION

The task of determining the position of a moving target poses many challenges, in particular in the fields of robotics, and control and estimation theory, see, e.g., [1], [2]. Real-world applications tend to lean on GPS-based systems, which can provide accurate position and velocity measurements, often improved with the help of real-time kinematic corrections. However, impracticality and unreliability of GPS signals in underwater and indoor environments, respectively, affect the development of robotic systems, which, naturally, shifts to more complex sensor integrating techniques. A recurring solution in the target tracking paradigm, henceforward designated as source localization problem, considers that the moving source emits signals encoding information about the source's absolute or relative motion. One can then feed the decoded information to algorithms whose filtered output is an estimate of the position of the source with respect to a given frame.

This well-known problem of source localization has been given a considerable amount of attention, with topics ranging from passive bearings-only observations, see e.g. [3], [4], [5], to range-only measurements, see e.g. [6] and [7], where the authors present a slight variation to the source localization problem by achieving circumnavigation. Whereas bearing measurements comprehend the passive paradigm, range observations imply an exchange of information between the source and the receiver, often based on synchronized interrogation schemes. However, velocity scaling and offsets, sensor position errors or synchronization clock drifts are drawbacks common to both paradigms, as evidenced in [8]. Correcting biases might prove useful in the design of estimation techniques, see, e.g., [9], [10], especially when biases stem from the nonlinear processing of non-perturbed measurements [11].

Other approaches to the problem of source localization rely on the use of multiple receivers, as shown in [12] and [13]. Moreover, besides bearings and ranges, localization techniques can take advantage of a myriad of sensors and observations, for instance multi-beam Doppler Velocity Logs [14], Doppler shifts [15] or wave energy [16].

Nonetheless, it is frequent to adapt the problem to search and rescue scenarios consisting of a stationary source and a mobile agent that aims to estimate its own relative position, see [17], where only the measured distance from the source is available. By having a mobile agent, one is allowed to describe trajectories that induce persistent excitation, therefore improving the performance of the estimators. Optimizing the maneuvers described by the receiver for bearings-only tracking is a topic addressed in [18]. In [19] it is reported a study on the optimal observer trajectories for bearings-only tracking by minimizing the trace of the Cramér-Rao lower bound. Similarly, but using range measurements instead, an optimal acoustic sensor placement technique for underwater tracking in three dimensions is presented in [20].

In this paper, a discrete-time linear system is designed for the problem of source localization based on discrete-time direction and velocity measurements. The work presented in the sequel builds on previous results obtained by the authors [21]. Also from the authors, see: [22], where the problem of source localization based on direction measurements was studied in a continuous-time setting; and [23], where multiple bearing measurements are considered as opposed to single reading, which, despite being theoretically more demanding, deems the proposed solution more attractive from a practical point of view. Notwithstanding, in this paper, strong forms of observability, namely uniform complete observability, are ensured through a condition that closely relates to the motion of the source. Most noticeably, in spite of a mild assumption concerning a discretization approach, no strong assumptions are made concerning the velocity of the source, apart from it being assumed bounded, whereby most practical trajectories are permitted. The problem addressed in this paper has also

J. Reis and C. Silvestre are with the Faculty of Science and Technology, University of Macau, Taipa, Macao (e-mail: joelreis@umac.mo; csilvestre@umac.mo).

P. Batista and P. Oliveira are with the Institute for Systems and Robotics, Instituto Superior Técnico, Universidade de Lisboa, Lisboa 1049-001, Portugal (e-mail: pbatista@isr.tecnico.ulisboa.pt; pjcro@isr.ist.utl.pt)

C. Silvestre is on leave from Instituto Superior Técnico, Universidade de Lisboa, Lisboa, Portugal.

This work was supported by the University of Macau Project MYRG2015-00127-FST and by the Fundação para a Ciência e a Tecnologia (FCT) through ISR under LARSyS UID/EEA/50009/2013 and through IDMEC under LAETA UID/EMS/50022/2013.

This article has been accepted for publication in a future issue of this journal, but has not been fully edited. Content may change prior to final publication. Citation information: DOI 10.1109/TAES.2018.2831118, IEEE Transactions on Aerospace and Electronic Systems

been considered in [24]. In a continuous-time framework, a nonlinear observer for position and velocity bias estimation is presented that achieves global practical stability.

In practice, bearing measurements consist in discrete-time samples, as is the case of underwater applications. This reality constitutes a challenge both in terms of observability analysis and filter design. In this paper, resorting to a discrete-time linear time-varying (DT-LTV) system, the design of an observer follows naturally from using classic estimation tools for linear systems. Thus, a Kalman filter is proposed that achieves globally exponentially stable (GES) error dynamics.

This paper is organized as follows: Section II describes the framework of the problem and outlines the system dynamics. The filter design and proofs regarding observability properties of the overall system are presented in Section III. Section IV includes simulation results along with Monte Carlo runs and a comparison with both the Extended Kalman Filter (EKF) and the Bayesian Cramér-Rao Lower Bound (BCRLB). Experimental results within the scope of an underwater mission scenario are shown in Section V. Finally, conclusions and a summary of the main results of this paper are reported in Section VI.

A. Notation

Throughout the paper, a bold symbol stands for a multi-dimensional variable. Accordingly, the symbol $\mathbf{0}$ denotes a matrix of zeros and $\mathbf{I}$ an identity matrix, both of appropriate dimensions. A block diagonal matrix is represented as diag($\mathbf{A}_1$,...,$\mathbf{A}_n$) and the set of unit vectors on $\mathbb{R}^3$ is denoted by $S(2)$. The determinant of a matrix is denoted by the operator $|\cdot|$. A positive-definite matrix $\mathbf{M}$ is identified as $\mathbf{M} \succ \mathbf{0}$. In $\mathbb{R}^3$, the skew-symmetric matrix of a generic vector $\mathbf{a} \in \mathbb{R}^3$ is defined as $\mathbf{S}(\mathbf{a})$, such that for another generic vector $\mathbf{b} \in \mathbb{R}^3$ one has $\mathbf{a} \times \mathbf{b} = \mathbf{S}(\mathbf{a})\mathbf{b}$, where

$$\mathbf{S}(\mathbf{a}) = \begin{bmatrix} 0 & -a_z & a_y \\ a_z & 0 & -a_x \\ -a_y & a_x & 0 \end{bmatrix}.$$

Finally, for convenience, the transpose operator is denoted by the superscript $(\cdot)^T$.

II. PROBLEM STATEMENT

Consider a mission scenario wherein a moving source describes a trajectory whose evolution in time is unknown. Let $\mathbf{s}_k \in \mathbb{R}^3$ be the position of the source at time $t = t_k \in \mathbb{R}$, with $t_{k+1} = t_k + T_k$, where $k \in \mathbb{N}_0$ is the time index, and T_k is the sampling time, which is assumed not constant. On the other hand, if $T_k = T$, for all k, then $t_k = t_0 + kT$, where $t_0 > 0$ corresponds to the initial time. At time $t = t_k$, the source, whose position one aims to estimate, moves with inertial velocity given by $\mathbf{v}_k \in \mathbb{R}^3$. Suppose that, at each sampling instant, one has access to readings of this inertial source velocity, denoted by $\mathbf{v}_k^m \in \mathbb{R}^3$ (superscript m stands for *measurement*). The latter are corrupted by an unknown constant inertial velocity bias, denoted by $\mathbf{b}_k \in \mathbb{R}^3$, such that $\mathbf{v}_k^m = \mathbf{v}_k - \mathbf{b}_k$, for all k. Furthermore, assume that the direction of the source relatively to the origin of the inertial frame is also measured, and given by

$$\mathbf{d}_k = \frac{\mathbf{s}_k}{\|\mathbf{s}_k\|} \in S(2). \tag{1}$$

For the continuous-time case, the evolution of the source position is computed by integrating the source velocity. Solving this integral is equivalent to solve an ordinary first order differential equation with a given initial value. The final solution for the discrete-time case is well approximated, under certain conditions, by the explicit first order Euler method, which motivates the following mild assumption:

Assumption 1. *The motion described by the source is such that*

$$\forall\ t_k \le t \le t_{k+1} : \int_{t_k}^{t} \mathbf{v}(\sigma) d\sigma = (t - t_k)\mathbf{v}_k. \tag{2}$$

Hence, the velocity is assumed to remain constant during the sampling interval.

This is a common assumption. Naturally, it holds stronger when considering short sampling intervals and/or slow maneuvers by the source, as is the case of most underwater robotic operations. From (2), the evolution of the source position is given by

$$\mathbf{s}_{k+1} = \mathbf{s}_k + T_k \mathbf{v}_k. \tag{3}$$

Thus, the nominal nonlinear discrete-time system dynamics for source localization with velocity bias estimation can be written as

$$\begin{cases} \mathbf{s}_{k+1} = \mathbf{s}_k + T_k \mathbf{v}_k \\ \mathbf{b}_{k+1} = \mathbf{b}_k \\ \mathbf{d}_k = \mathbf{s}_k \|\mathbf{s}_k\|^{-1} \\ \mathbf{v}_k^m = \mathbf{v}_k - \mathbf{b}_k \end{cases}. \tag{4}$$

Using the dynamics in (4), the discrete propagation established in (3) can be rewritten as

$$\mathbf{s}_{k+1} = \mathbf{s}_k + T_k \mathbf{b}_k + T_k \mathbf{v}_k^m. \tag{5}$$

To illustrate a practical situation, suppose the source is an autonomous underwater vehicle (AUV) equipped with an Inertial Measurement Unit (IMU) in addition to an Acoustic Doppler current profiler. The latter provides velocity readings, taken with respect to the fluid, which when combined with the IMU outputs allow to compute a velocity expressed in the inertial frame, i.e. $\mathbf{v}_k^m$. Suppose also that the velocity of the fluid (i.e. the ocean current) is given by $\mathbf{b}_k$, which is assumed constant, and that the source emits an acoustic signal which encapsulates $\mathbf{v}_k^m$. In turn, let there be at the origin of the inertial frame a receiver equipped, for example, with an Ultra-Short BaseLine (USBL) acoustic positioning system. Upon signal detection, the receiver computes a bearing and simultaneously decodes the sampled signal, thus unwrapping the vector $\mathbf{v}_k^m$ that had been coded before.

In short, the problem of source localization considered in this paper is that of designing a filter with GES error dynamics for the nominal nonlinear system (4), considering also additive process and sensor noises.

In order to validate some of the results derived in the remainder of this paper, the following assumption is made:

Assumption 2. *For all k, the motion kinematics of the source is such that*

$$\mathbf{d}_k^T \mathbf{d}_{k+1} > 0,$$

and all direction measurements are well defined and norm-bounded by construction, implying, from (1), *that* $\mathbf{s}_k \neq \mathbf{0}$.

Notice that this is a mild assumption, as a variation of 90 degrees or more of direction measurements between consecutive instants is not expected. Furthermore, the source cannot physically overlap the receiver.

III. SOURCE LOCALIZATION FILTER DESIGN

In this paper, sampling times can change over time and a passive tracking paradigm is considered where the velocity measurements correspond to the movement of the source with respect to an inertial reference frame. By regarding the velocity of the source as an external input of the system, one can design a linear system that mimics both the dynamics and observations as presented in previous work by the authors [21].

A. System Augmentation

This section details the procedures in obtaining a linear system useful for the design of an estimator for the nonlinear discrete-time system (4). In summary, the range to the source is added to the system state vector, whereby the output, based on this new augmented vector, is redesigned to become linear. Moreover, velocity measurements are regarded as inputs to the system, which allows to write the overall system dynamics as a function of both the whole state vector and the system input.

Define as system state

$$\begin{cases} \mathbf{x}_{1,k} := \mathbf{s}_k \\ \mathbf{x}_{2,k} := \mathbf{b}_k \\ x_{3,k} := \|\mathbf{s}_k\| \end{cases},$$

where the scalar $x_{3,k}$ corresponds to the distance from the source to the origin of the frame. Then, from (4), the evolution of the first two states is simply given by

$$\begin{cases} \mathbf{x}_{1,k+1} = \mathbf{x}_{1,k} + T_k \mathbf{x}_{2,k} + T_k \mathbf{u}_k \\ \mathbf{x}_{2,k+1} = \mathbf{x}_{2,k} \end{cases} \tag{6a}$$

with $\mathbf{u}_k := \mathbf{v}_k^m$. The less intuitive state propagation concerns $x_{3,k}$, but from (1) it is possible to write

$$\mathbf{d}_{k+1} x_{3,k+1} = \mathbf{x}_{1,k+1}. \tag{7}$$

Since $\mathbf{d}_{k+1}^T \mathbf{d}_{k+1} = \|\mathbf{d}_{k+1}\|^2 = 1$, the inner product of both sides in (7) with $\mathbf{d}_{k+1}$ yields

$$x_{3,k+1} = \mathbf{d}_{k+1}^T \mathbf{x}_{1,k+1}. \tag{8}$$

Next, substitute (6a) in (8) and notice that $\mathbf{x}_{1,k} = \mathbf{d}_k x_{3,k}$, which allows to rewrite (8) as

$$x_{3,k+1} = \mathbf{d}_{k+1}^T \mathbf{d}_k x_{3,k} + T_k \mathbf{d}_{k+1}^T \mathbf{x}_{2,k} + T_k \mathbf{d}_{k+1}^T \mathbf{u}_k.$$

This is an interesting result in the sense that it expresses $x_{3,k+1}$ as a linear function of its previous state, $x_{3,k}$, in addition to an external input.

Define now the augmented state vector

$$\mathbf{x}_k := \begin{bmatrix} \mathbf{x}_{1,k} \\ \mathbf{x}_{2,k} \\ x_{3,k} \end{bmatrix} \in \mathbb{R}^{3+3+1}.$$

From (7), the following holds:

$$\mathbf{0} = \mathbf{x}_{1,k+1} - x_{3,k+1} \mathbf{d}_{k+1}, \tag{9}$$

whereby a vector of virtual null measurements is taken in place of explicit direction measurements. Hence, with respect to the nominal nonlinear dynamics in (4), by considering (9), by discarding the original nonlinear output (1), and by regarding the velocity measurements as an input (instead of a state) to the system, one can write the DT-LTV system

$$\begin{cases} \mathbf{x}_{k+1} = \mathbf{A}_k \mathbf{x}_k + \mathbf{B}_k \mathbf{u}_k \\ \mathbf{y}_{k+1} = \mathbf{C}_{k+1} \mathbf{x}_{k+1} \end{cases}, \tag{10}$$

where the dynamics matrix $\mathbf{A}_k \in \mathbb{R}^{7 \times 7}$ is given by

$$\mathbf{A}_k = \begin{bmatrix} \mathbf{I} & T_k \mathbf{I} & \mathbf{0} \\ \mathbf{0} & \mathbf{I} & \mathbf{0} \\ \mathbf{0} & T_k \mathbf{d}_{k+1}^T & \mathbf{d}_{k+1}^T \mathbf{d}_k \end{bmatrix}, \tag{11}$$

the input matrix $\mathbf{B}_k \in \mathbb{R}^{7 \times 3}$ is written as

$$\mathbf{B}_k = \begin{bmatrix} T_k \mathbf{I} \\ \mathbf{0} \\ T_k \mathbf{d}_{k+1}^T \end{bmatrix},$$

and, finally, the observations matrix $\mathbf{C}_k \in \mathbb{R}^{3 \times 7}$ can be written as

$$\mathbf{C}_k = \begin{bmatrix} \mathbf{I} & \mathbf{0} & -\mathbf{d}_k \end{bmatrix}.$$

The following lemma is useful in the sequel.

Lemma 1. *Three vectors* $\mathbf{v}_1, \mathbf{v}_2, \mathbf{v}_3 \in \mathbb{R}^3$ *are linearly independent if and only if*

$$\begin{vmatrix} \mathbf{v}_1^T \mathbf{v}_1 & \mathbf{v}_1^T \mathbf{v}_2 & \mathbf{v}_1^T \mathbf{v}_3 \\ \mathbf{v}_2^T \mathbf{v}_1 & \mathbf{v}_2^T \mathbf{v}_2 & \mathbf{v}_2^T \mathbf{v}_3 \\ \mathbf{v}_3^T \mathbf{v}_1 & \mathbf{v}_3^T \mathbf{v}_2 & \mathbf{v}_3^T \mathbf{v}_3 \end{vmatrix} > 0.$$

Proof. Define $\mathbf{V} := [\mathbf{v}_1 \ \mathbf{v}_2 \ \mathbf{v}_3] \in \mathbb{R}^{3 \times 3}$. The three vectors are linearly independent if and only if $\text{rank}(\mathbf{V}) = 3$. The latter is verified if and only if $|\mathbf{V}| \neq 0$. In turn, this is true if and only if $|\mathbf{V}^T||\mathbf{V}| = |\mathbf{V}^T \mathbf{V}| > 0$. □

B. Observability analysis

Given k_0, $k_f > 0$, and letting $k_f \geq k_0 + 1$, if any initial state $\mathbf{x}_{k_0}$ can be uniquely determined from the sequences of inputs and outputs, $\{\mathbf{u}_{k_0}, \mathbf{u}_{k_1}, \ldots, \mathbf{u}_{k_f - 1}\}$ and $\{\mathbf{y}_{k_0}, \mathbf{y}_{k_1}, \ldots, \mathbf{y}_{k_f - 1}\}$, respectively, then the DT-LTV system (10) is said to be observable on $[k_0, k_f]$ ([25, Definition 25.8]). Therefore, the main concern lies in selecting the shortest interval for observability. The next theorem provides a necessary and sufficient condition for the observability criterion.

Theorem 1. *Under* Assumption 2, *and for any fixed* $k \geq k_0$, *the DT-LTV system* (10) *is observable on* $[k, k+3]$ *if and*

This article has been accepted for publication in a future issue of this journal, but has not been fully edited. Content may change prior to final publication. Citation information: DOI 10.1109/TAES.2018.2831118, IEEE Transactions on Aerospace and Electronic Systems

only if the set of vectors $\boldsymbol{\mathcal{D}} := \{\mathbf{d}_k, \mathbf{d}_{k+1}, \mathbf{d}_{k+2}\}$ *is linearly independent.*

Proof. From *Lemma* 1, and since $\|\mathbf{d}_k\| = 1$, it follows that the DT-LTV system (10) is observable if and only if

$$\begin{vmatrix} 1 & \mathbf{d}_k^T\mathbf{d}_{k+1} & \mathbf{d}_k^T\mathbf{d}_{k+2} \\ \mathbf{d}_{k+1}^T\mathbf{d}_k & 1 & \mathbf{d}_{k+1}^T\mathbf{d}_{k+2} \\ \mathbf{d}_{k+2}^T\mathbf{d}_k & \mathbf{d}_{k+2}^T\mathbf{d}_{k+1} & 1 \end{vmatrix} > 0,$$

which is equivalent to

$$2\mathbf{d}_k^T\mathbf{d}_{k+1}\mathbf{d}_k^T\mathbf{d}_{k+2}\mathbf{d}_{k+1}^T\mathbf{d}_{k+2} - \left(\mathbf{d}_k^T\mathbf{d}_{k+1}\right)^2 - \left(\mathbf{d}_k^T\mathbf{d}_{k+2}\right)^2 + 1 - \left(\mathbf{d}_{k+1}^T\mathbf{d}_{k+2}\right)^2 > 0. \tag{12}$$

In the remainder of this paper, (12) will be called the observability condition.

The proof of *Theorem* 1 resorts to the analysis of the observability matrix $\boldsymbol{\mathcal{O}}[k, k+3]$ associated with the pair $(\mathbf{A}_k, \mathbf{C}_k)$ on $[k,k+3]$, given by

$$\boldsymbol{\mathcal{O}}[k,k+3] = \begin{bmatrix} \mathbf{C}_k \\ \mathbf{C}_{k+1}\mathbf{A}_k \\ \mathbf{C}_{k+2}\mathbf{A}_{k+1}\mathbf{A}_k \end{bmatrix} \in \mathbb{R}^{9\times 7}. \tag{13}$$

The DT-LTV system 10 is observable on $[k,k+3]$ if and only if (13) is full rank. Let $\mathbf{c} = [\mathbf{c}_1^T \; \mathbf{c}_2^T \; c_3]^T \in \mathbb{R}^7$ be a unit vector, with $\mathbf{c}_1,\mathbf{c}_2 \in \mathbb{R}^3$ and $c_3 \in \mathbb{R}$, and write

$$\boldsymbol{\mathcal{O}}[k,k+3]\mathbf{c} = \begin{bmatrix}\boldsymbol{\mathcal{O}}_1^T & \boldsymbol{\mathcal{O}}_2^T & \boldsymbol{\mathcal{O}}_3^T\end{bmatrix}^T \in \mathbb{R}^{3+3+3},$$

with

$$\boldsymbol{\mathcal{O}}_1 := \mathbf{c}_1 - \mathbf{d}_k c_3, \tag{14}$$

$$\boldsymbol{\mathcal{O}}_2 := \mathbf{c}_1 - T_k\mathbf{S}^2(\mathbf{d}_{k+1})\mathbf{c}_2 - \left(\mathbf{d}_{k+1}^T\mathbf{d}_k\right)\mathbf{d}_{k+1}c_3, \tag{15}$$

and

$$\boldsymbol{\mathcal{O}}_3 := \mathbf{c}_1 + \left[T_k\mathbf{I} - T_{k+1}\mathbf{S}^2(\mathbf{d}_{k+2})\right]\mathbf{c}_2 - \left(\mathbf{d}_{k+2}^T\mathbf{d}_{k+1}\right)\left[T_k\left(\mathbf{d}_{k+1}^T\mathbf{c}_2\right)\mathbf{d}_{k+2} + c_3\left(\mathbf{d}_k^T\mathbf{d}_{k+1}\right)\mathbf{d}_{k+2}\right], \tag{16}$$

where the projection operator $\mathbf{S}^2(\mathbf{a}) = \mathbf{a}\mathbf{a}^T - \mathbf{I}$, for $\|\mathbf{a}\| = 1$, was used.

To prove that (12) is a necessary condition, suppose first that it does not hold, i.e.

$$2\mathbf{d}_k^T\mathbf{d}_{k+1}\mathbf{d}_k^T\mathbf{d}_{k+2}\mathbf{d}_{k+1}^T\mathbf{d}_{k+2} - \left(\mathbf{d}_k^T\mathbf{d}_{k+1}\right)^2 - \left(\mathbf{d}_k^T\mathbf{d}_{k+2}\right)^2 + 1 - \left(\mathbf{d}_{k+1}^T\mathbf{d}_{k+2}\right)^2 = 0. \tag{17}$$

This is to say, by contraposition, that (17) implies that the DT-LTV system (10) is not observable. Consider now two different cases:

- $\mathbf{d}_{k+1} = \mathbf{d}_{k+2}$

Let $\mathbf{c}_1 = \mathbf{0}$, $\mathbf{c}_2 = \mathbf{d}_{k+2}$, and $c_3 = 0$. Since $\mathbf{S}^2(\mathbf{a})\mathbf{a} = \mathbf{0}$, substituting $\mathbf{c}$ in (14)-(16) results in $\boldsymbol{\mathcal{O}}[k,k+3]\mathbf{c} = \mathbf{0}$, which means that the observability matrix is not full rank and hence the DT-LTV system (10) is not observable.

- $\mathbf{d}_{k+1} \neq \mathbf{d}_{k+2}$

Let $\mathbf{c}_1 = \mathbf{d}_k c_3$,

$$\mathbf{c}_2 = \alpha\frac{c_3}{T_k + T_{k+1}}\mathbf{d}_{k+1} + \frac{c_3}{T_k}\mathbf{S}^2(\mathbf{d}_{k+1})\mathbf{d}_k, \tag{18}$$

with

$$\alpha := -\frac{\mathbf{d}_k^T\mathbf{d}_{k+1}}{1-\left(\mathbf{d}_{k+1}^T\mathbf{d}_{k+2}\right)^2} - \frac{T_{k+1}}{T_k}\frac{\left(\mathbf{d}_k^T\mathbf{d}_{k+2}\right)\left(\mathbf{d}_{k+1}^T\mathbf{d}_{k+2}\right)}{1-\left(\mathbf{d}_{k+1}^T\mathbf{d}_{k+2}\right)^2} + \left(1+\frac{T_{k+1}}{T_k}\right)\frac{\left(\mathbf{d}_k^T\mathbf{d}_{k+1}\right)\left(\mathbf{d}_{k+1}^T\mathbf{d}_{k+2}\right)^2}{1-\left(\mathbf{d}_{k+1}^T\mathbf{d}_{k+2}\right)^2}, \tag{19}$$

and $c_3 \neq 0$. Again, substitute the unit vector $\mathbf{c}$ in (14)-(16). The terms $\boldsymbol{\mathcal{O}}_1$ and $\boldsymbol{\mathcal{O}}_2$ are easily shown to be zero, while $\boldsymbol{\mathcal{O}}_3$, after tedious computations, can be written as

$$\begin{aligned}\boldsymbol{\mathcal{O}}_3 = & \frac{c_3}{1-\left(\mathbf{d}_{k+1}^T\mathbf{d}_{k+2}\right)^2}\frac{T_{k+1}}{T_k}\Big(\mathbf{d}_k\left[\left(\mathbf{d}_{k+2}^T\mathbf{d}_{k+1}\right)^2 - 1\right] \\ & + \mathbf{d}_{k+1}\left[\left(\mathbf{d}_{k+1}^T\mathbf{d}_k\right) - \left(\mathbf{d}_{k+2}^T\mathbf{d}_k\right)\left(\mathbf{d}_{k+2}^T\mathbf{d}_{k+1}\right)\right] \\ & + \mathbf{d}_{k+2}\left[\left(\mathbf{d}_{k+2}^T\mathbf{d}_k\right) - \left(\mathbf{d}_{k+2}^T\mathbf{d}_{k+1}\right)\left(\mathbf{d}_{k+1}^T\mathbf{d}_k\right)\right]\Big).\end{aligned} \tag{20}$$

Now, since (17) holds, i.e. $\boldsymbol{\mathcal{D}}$ is linearly dependent, there are $a,b \in \mathbb{R}$ such that $\mathbf{d}_k = a\mathbf{d}_{k+1} + b\mathbf{d}_{k+2}$. Substituting this in (20) allows to show that $\boldsymbol{\mathcal{O}}[k,k+3]\mathbf{c} = \mathbf{0}$, therefore the observability matrix is not full rank and hence the DT-LTV system (10) is not observable. Thus, it has been shown that if (12) does not hold, the DT-LTV system (10) is not observable on $[k, k+3]$. By contraposition, if the DT-LTV system (10) is observable on $[k, k+3]$, then (12) must hold, thus concluding the proof of necessity.

The proof of sufficiency follows by contraposition as well. Suppose that the DT-LTV (10) is not observable, which means there exists a unit vector $\mathbf{c}$ such that $\boldsymbol{\mathcal{O}}[k,k+3]\mathbf{c} = \mathbf{0}$. In turn, this must imply that the observability condition (12) cannot hold. From (14) it must be

$$\mathbf{c}_1 = \mathbf{d}_k c_3. \tag{21}$$

Consider first that $c_3 = 0$. Then, from (21) it must be also $\mathbf{c}_1 = \mathbf{0}$. Substituting that in (15) allows to conclude that it must be $\mathbf{c}_2 = \pm\mathbf{d}_{k+1}$. Substituting $\mathbf{c}_1 = \mathbf{0}$, $\mathbf{c}_2 = \pm\mathbf{d}_{k+1}$, and $c_3 = 0$ in (16) gives

$$\left(T_k + T_{k+1}\right)\mathbf{S}^2(\mathbf{d}_{k+2})\mathbf{d}_{k+1} = \mathbf{0}, \tag{22}$$

whose only solution, under *Assumption* 2 , is $\mathbf{d}_{k+1} = \mathbf{d}_{k+2}$. With $\mathbf{d}_{k+1} = \mathbf{d}_{k+2}$ it follows that the set of vectors is not linearly independent. Hence, it has been shown that if a unit vector $\mathbf{c}$ exists, with $c_3 = 0$, such that $\boldsymbol{\mathcal{O}}[k,k+3]\mathbf{c} = \mathbf{0}$, then (12) cannot hold. Consider now $c_3 \neq 0$ and substitute (21) in (15) to obtain

$$T_k\mathbf{S}^2(\mathbf{d}_{k+1})\mathbf{c}_2 = c_3\left[\mathbf{d}_k - \left(\mathbf{d}_k^T\mathbf{d}_{k+1}\right)\mathbf{d}_{k+1}\right]. \tag{23}$$

Suppose first that $\mathbf{c}_2 = \mathbf{0}$. Then, from (23) it results

$$c_3\mathbf{S}^2(\mathbf{d}_{k+1})\mathbf{d}_k = \mathbf{0},$$

whose only solution, with $c_3 \neq 0$ and under *Assumption* 2, is $\mathbf{d}_k = \mathbf{d}_{k+1}$, which means that the set of vectors $\boldsymbol{\mathcal{D}}$ is not linearly independent. Consider now $c_3 \neq 0$, $\mathbf{c}_2 \neq \mathbf{0}$, and decompose $\mathbf{c}_2$ as

$$\mathbf{c}_2 = \frac{\beta}{T_k + T_{k+1}}\mathbf{d}_{k+1} + \mathbf{c}_2', \tag{24}$$

where $\beta \in \mathbb{R}$ and $\mathbf{c}_2' \in \mathbb{R}^3$ is orthogonal to $\mathbf{d}_{k+1}$. Substituting (24) in (23) implies

$$\mathbf{c}_2' = \frac{c_3}{T_k}\mathbf{S}^2(\mathbf{d}_{k+1})\mathbf{d}_k,$$

which means that it must be

$$\mathbf{c}_2 = \frac{\beta}{T_k + T_{k+1}}\mathbf{d}_{k+1} + \frac{c_3}{T_k}\mathbf{S}^2(\mathbf{d}_{k+1})\mathbf{d}_k, \tag{25}$$

for some $\beta \in \mathbb{R}$. Next, substitute (21) and (25) in (16) and apply further simplifications in order to get

$$\begin{aligned} &-\left(1+\frac{T_{k+1}}{T_k}\right)\left(\mathbf{d}_k^T\mathbf{d}_{k+1}\right)c_3\mathbf{S}^2(\mathbf{d}_{k+2})\mathbf{d}_{k+1} \\ &+\frac{T_{k+1}}{T_k}c_3\mathbf{S}^2(\mathbf{d}_{k+2})\mathbf{d}_k - \beta\mathbf{S}^2(\mathbf{d}_{k+2})\mathbf{d}_{k+1} = \mathbf{0}. \end{aligned} \tag{26}$$

Notice that (26) is a sum of terms projected onto a plane orthogonal to $\mathbf{d}_{k+2}$. Consequently, the inner product of the left side of (26) with $\mathbf{d}_{k+2}$ is always null, regardless of β. Moreover, (26) is satisfied if and only if the inner product of the left side of (26) with the remaining two direction vectors is null. Thus, by computing the inner product of both sides of (26) with $\mathbf{d}_{k+1}$ one can write

$$\begin{aligned} \beta\left\{1-\left(\mathbf{d}_{k+1}^T\mathbf{d}_{k+2}\right)^2\right\} = \Big\{&-\frac{T_{k+1}}{T_k}\left(\mathbf{d}_k^T\mathbf{d}_{k+2}\right)\left(\mathbf{d}_{k+1}^T\mathbf{d}_{k+2}\right) \\ &-\mathbf{d}_k^T\mathbf{d}_{k+1} + \left(1+\frac{T_{k+1}}{T_k}\right)\left(\mathbf{d}_k^T\mathbf{d}_{k+1}\right)\left(\mathbf{d}_{k+1}^T\mathbf{d}_{k+2}\right)^2\Big\}c_3. \end{aligned} \tag{27}$$

Since $\mathbf{c}_2 \neq \mathbf{0}$ is the case under analysis, from (27) one concludes that $\mathbf{d}_k \neq \mathbf{d}_{k+1}$. On the other hand, if $\mathbf{d}_k = \mathbf{d}_{k+1}$, then the set of vectors $\boldsymbol{\mathcal{D}}$ is not linearly independent. Suppose now that $\mathbf{d}_{k+1} \neq \mathbf{d}_{k+2}$. It follows from (27) that

$$\beta = \alpha c_3, \tag{28}$$

with α as defined in (19). Substituting (28) in (26), computing the inner product of both sides of (26) with $\mathbf{d}_k$, and simplifying allows us to conclude that (17) holds, and hence the set of vectors $\boldsymbol{\mathcal{D}}$ is not linearly independent. On the other hand, if $\mathbf{d}_{k+1} = \mathbf{d}_{k+2}$, then (17) also holds, yielding the same conclusion. Thus, it has been shown that if a unit vector $\mathbf{c}$ exists, with $c_3 \neq 0$, such that $\boldsymbol{\mathcal{O}}[k,k+3]\mathbf{c} = \mathbf{0}$, then the set of vectors $\boldsymbol{\mathcal{D}}$ is not linearly independent. But that had already been shown for $c_3 = 0$. Hence, if a unit vector $\mathbf{c}$ exists such that $\boldsymbol{\mathcal{O}}[k,k+3]\mathbf{c} = \mathbf{0}$ or, equivalently, if the DT-LTV system (10) is not observable, then the set of vectors $\boldsymbol{\mathcal{D}}$ is not linearly independent. By contraposition, if the set of vectors $\boldsymbol{\mathcal{D}}$ is linearly independent, the DT-LTV system (10) is observable, thus concluding the proof of sufficiency. □

Corollary 1. *If the observability condition* (12) *holds, then the initial state* $\mathbf{x}_k$ *is uniquely determined by the input and output sequences* $\{\mathbf{u}_k,\mathbf{u}_{k+1},\mathbf{u}_{k+2}\}$ *and* $\{\mathbf{y}_k,\mathbf{y}_{k+1},\mathbf{y}_{k+2}\}$*, respectively.*

Before proceeding, it is important to stress that the nonlinearities presented in the original nonlinear discrete-time system (4) were replaced by a set of virtual null measurements, as indicated by (9). In addition, there is nothing imposing the initial condition of (4) to match that of the augmented DT-LTV system (10). Consequently, regarding the observability properties derived for the DT-LTV system (10), care must be taken when extrapolating the previous conclusions to the nonlinear discrete-time system (4). The following theorem addresses this issue.

Theorem 2. *Consider* Assumption *2 and suppose that the observability condition* (12) *holds. Then:*

1) *the initial condition of* (10) *matches that of* (4)*, i.e.*

$$\begin{cases} \mathbf{x}_{1,k_0} = \mathbf{s}_{k_0} \\ \mathbf{x}_{2,k_0} = \mathbf{b}_{k_0} \\ x_{3,k_0} = \|\mathbf{s}_{k_0}\| \end{cases}; \tag{29}$$

2) *the discrete-time nonlinear system 4 is observable in the sense that, given the system input* $\mathbf{u}_k$ *and the output* $\mathbf{d}_k$*, for* $k = k_0,\ k_0+1,\ k_0+2$*, its initial condition is uniquely determined; and*
3) *an observer for the DT-LTV system* (10) *with GES error dynamics is also an observer for the nonlinear system* (4)*, whose error converges exponentially fast to zero for all initial conditions.*

Proof. According to *Theorem* 1, the initial condition of the DT-LTV system (10) is uniquely determined by the corresponding system output and input for $k = k_0,\ k_0+1,\ k_0+2$. Proving 1) consists in comparing the outputs of both the nonlinear system (4) and the DT-LTV system (10) as a function of their initial state, and then show that (29) explains the system output, which is zero for this particular DT-LTV system, as indicated by (9). First, let $\mathbf{x}_{k_0} := [\mathbf{x}_{1,k_0}^T\ \mathbf{x}_{2,k_0}^T\ x_{3,k_0}]^T$. Write the output of (10) as function of the initial state $\mathbf{x}_{k_0}$, resulting in

$$\begin{aligned} \begin{bmatrix}\mathbf{y}_{k_0}\\ \mathbf{y}_{k_0+1}\\ \mathbf{y}_{k_0+2}\end{bmatrix} = \mathbf{0} = &\begin{bmatrix}\mathbf{C}_{k_0}\\ \mathbf{C}_{k_0+1}\mathbf{A}_{k_0}\\ \mathbf{C}_{k_0+2}\mathbf{A}_{k_0+1}\mathbf{A}_{k_0}\end{bmatrix}\mathbf{x}_{k_0} \\ &+\begin{bmatrix}\mathbf{0}\\ \mathbf{C}_{k_0+1}\mathbf{B}_{k_0}\\ \mathbf{C}_{k_0+2}\mathbf{A}_{k_0+1}\mathbf{B}_{k_0}\end{bmatrix}\mathbf{u}_{k_0} + \begin{bmatrix}\mathbf{0}\\ \mathbf{0}\\ \mathbf{C}_{k_0+2}\mathbf{B}_{k_0+1}\end{bmatrix}\mathbf{u}_{k_0+1}. \end{aligned} \tag{30}$$

In light of *Theorem* 1, since the DT-LTV system (10) is observable, one needs only to show that the initial condition (29) explains (30). If it does, then, because the DT-LTV system is observable, there can be only one initial condition to explain the system output and, therefore, (29) is unique. Hence, substitute (29) in (30) to obtain the three following equations:

$$\mathbf{0} = \mathbf{s}_{k_0} - \mathbf{d}_{k_0}\|\mathbf{s}_{k_0}\|; \tag{31}$$

$$\mathbf{0} = \mathbf{s}_{k_0} - \mathbf{S}^2(\mathbf{d}_{k_0+1})T_{k_0}\left(\mathbf{b}_{k_0}+\mathbf{u}_{k_0}\right) - \mathbf{d}_{k_0+1}\mathbf{d}_{k_0+1}^T\mathbf{d}_{k_0}\|\mathbf{s}_{k_0}\|; \tag{32}$$

and, finally,

$$\begin{aligned} \mathbf{0} = \mathbf{s}_{k_0} + T_{k_0}\left(\mathbf{b}_{k_0}+\mathbf{u}_{k_0}\right) - T_{k_0+1}\mathbf{S}^2(\mathbf{d}_{k_0+2})\left(\mathbf{b}_{k_0}+\mathbf{u}_{k_0+1}\right) \\ - \mathbf{d}_{k_0+2}\mathbf{d}_{k_0+2}^T\mathbf{d}_{k_0+1}\mathbf{d}_{k_0+1}^T\left(\mathbf{d}_{k_0}\|\mathbf{s}_{k_0}\| + T_{k_0}\left(\mathbf{b}_{k_0}+\mathbf{u}_{k_0}\right)\right). \end{aligned} \tag{33}$$

From (1) it follows that (31) is true. In turn, according also to (1), equation (32) can be rewritten as

$$\mathbf{0} = -\mathbf{S}^2(\mathbf{d}_{k_0+1})\left(\mathbf{s}_{k_0} + T_{k_0}\left(\mathbf{b}_{k_0}+\mathbf{u}_{k_0}\right)\right),$$

This article has been accepted for publication in a future issue of this journal, but has not been fully edited. Content may change prior to final publication. Citation information: DOI 10.1109/TAES.2018.2831118, IEEE Transactions on Aerospace and Electronic Systems

which, according to (5), yields $\mathbf{0} = -\mathbf{S}^2(\mathbf{d}_{k_0+1})\mathbf{s}_{k_0+1}$. As $\mathbf{s}_{k_0+1}$ is aligned with $\mathbf{d}_{k_0+1}$, then (32) must also be true. Lastly, after simplifications, equation (33) becomes

$$\mathbf{0} = -\mathbf{S}^2(\mathbf{d}_{k_0+2})\left(\mathbf{s}_{k_0+1} + T_{k_0+1}\left(\mathbf{b}_{k_0} + \mathbf{u}_{k_0+1}\right)\right).$$

Once again resorting to (5), and as $\mathbf{b}_{k_0} = \mathbf{b}_{k_0+1}$, the previous result yields $\mathbf{0} = -\mathbf{S}^2(\mathbf{d}_{k_0+2})\mathbf{s}_{k_0+2}$. Likewise, as $\mathbf{s}_{k_0+2}$ is aligned with $\mathbf{d}_{k_0+2}$, (33) must be true, thus concluding the proof of 1). Regarding 2), in *Theorem* 1 the initial condition of the DT-LTV system (10) was shown to be uniquely determined. Accordingly, due to the correspondence between both systems, the initial condition of (4) is also uniquely determined, and thus the proof of 2) is concluded. The proof of 3) follows naturally: the estimates of an observer with GES error dynamics applied to (10) approach the true state globally exponentially fast. Notwithstanding, this true state has been shown to correspond to the state of the nonlinear discrete-time system (4), therefore those estimates approach the state of (4) globally exponentially fast, thus completing the proof. □

The previous analysis considered the shortest interval for observability. The observability condition (12) expresses that, considering three time instants, the direction vectors ought to span $\mathbb{R}^3$. This is an expected result in terms of compulsory motion, as for systems with linear dynamics the direction measurements alone cannot render the system observable [26]. Nonetheless, if larger intervals are considered, this condition can be relaxed, in particular the direction measurements need only to span $\mathbb{R}^2$. This leads to a new observability condition, which is enclosed in the following theorem.

Theorem 3. *Consider the set of four consecutive and coplanar direction vectors* $\mathcal{D}^+ := \{\mathbf{d}_k,\mathbf{d}_{k+1},\mathbf{d}_{k+2},\mathbf{d}_{k+3}\}$ *and let there be constants* a, b, $c \in \mathbb{R}$ *such that*

$$a\mathbf{d}_k + b\mathbf{d}_{k+1} + c\mathbf{d}_{k+2} = 0. \tag{34}$$

The DT-LTV system (10) *is observable on* $[k, k+4]$ *if and only if* $\mathbf{d}_k$, $\mathbf{d}_{k+1}$, $\mathbf{d}_{k+2}$ *are all non-collinear and, for* $a \neq 0$,

$$\mathbf{d}_{k+3} \neq \begin{cases} \dfrac{b}{ad}\dfrac{T_{k+2}\mathbf{d}_{k+1}}{T_k+T_{k+1}} + \dfrac{c}{ad}\dfrac{T_{k+1}+T_{k+2}}{T_k}\mathbf{d}_{k+2}, & \text{if } \mathbf{d}_{k+1} \neq \mathbf{d}_{k+2} \\ \mathbf{d}_{k+1}, & \text{if } \mathbf{d}_{k+1} = \mathbf{d}_{k+2} \end{cases} \tag{35}$$

where $d \in \mathbb{R}\backslash\{0\}$ is a normalizing constant such that the right side of (35) has always unit norm.

Proof. The proof follows similar steps to those of *Theorem* 1, only this time resorting to the analysis of the observability matrix $\mathcal{O}[k,k+4]$. Start by writing

$$\mathcal{O}[k,k+4]\mathbf{c} = \begin{bmatrix}\mathcal{O}_1^T & \mathcal{O}_2^T & \mathcal{O}_3^T & \mathcal{O}_4^T\end{bmatrix}^T \in \mathbb{R}^{3+3+3+3},$$

where $\mathcal{O}_1$, $\mathcal{O}_2$ and $\mathcal{O}_3$ are the same as in (14)-(16), respectively, $\mathcal{O}_4$ is given by

$$\begin{aligned}\mathcal{O}_4 :=& \mathbf{c}_1 - \mathbf{d}_{k+3}\mathbf{d}_{k+3}^T\mathbf{d}_{k+2}\mathbf{d}_{k+2}^T\mathbf{d}_{k+1}\mathbf{d}_{k+1}^T\mathbf{d}_k c_3 \\ &+ \big[(T_k+T_{k+1}+T_{k+2})\mathbf{I} - T_k\mathbf{d}_{k+3}\mathbf{d}_{k+3}^T\mathbf{d}_{k+2}\mathbf{d}_{k+2}^T\mathbf{d}_{k+1}\mathbf{d}_{k+1}^T \\ &- T_{k+1}\mathbf{d}_{k+3}\mathbf{d}_{k+3}^T\mathbf{d}_{k+2}\mathbf{d}_{k+2}^T - T_{k+2}\mathbf{d}_{k+3}\mathbf{d}_{k+3}^T\big]\,\mathbf{c}_2,\end{aligned} \tag{36}$$

and $\mathbf{c} = [\mathbf{c}_1^T\ \mathbf{c}_2^T\ c_3]^T \in \mathbb{R}^7$ is again a unit vector, with $\mathbf{c}_1,\mathbf{c}_2 \in \mathbb{R}^3$ and $c_3 \in \mathbb{R}$. To prove necessity, suppose that $\mathbf{d}_k$, $\mathbf{d}_{k+1}$, $\mathbf{d}_{k+2}$ are all collinear or that (35) does not hold, i.e.

$$\mathbf{d}_{k+3} = \begin{cases} \dfrac{b}{ad}\dfrac{T_{k+2}\mathbf{d}_{k+1}}{T_k+T_{k+1}} + \dfrac{c}{ad}\dfrac{T_{k+1}+T_{k+2}}{T_k}\mathbf{d}_{k+2}, & \text{if } \mathbf{d}_{k+1} \neq \mathbf{d}_{k+2} \\ \mathbf{d}_{k+1}, & \text{if } \mathbf{d}_{k+1} = \mathbf{d}_{k+2} \end{cases}.$$

Consider now three different cases:

- $\mathbf{d}_k = \mathbf{d}_{k+1} = \mathbf{d}_{k+2}$

Let $\mathbf{c}_1 = \mathbf{d}_k c_3$ and $\mathbf{c}_2 = -\mathbf{d}_k c_3/\left(T_k + T_{k+1} + T_{k+2}\right)$. Hence, regardless of $\mathbf{d}_{k+3}$, $\mathcal{O}[k,k+4]\mathbf{c} = \mathbf{0}$, which means that for the DT-LTV system (10) to be observable $\mathbf{d}_k$, $\mathbf{d}_{k+1}$, $\mathbf{d}_{k+2}$ must be all non-collinear.

- $\mathbf{d}_k \neq \mathbf{d}_{k+1} = \mathbf{d}_{k+2}$

Choose $\mathbf{c} = [\mathbf{0}\ \pm\mathbf{d}_{k+2}^T\ 0]^T$. It follows from *Theorem* 1 that $\mathcal{O}_1 = \mathcal{O}_2 = \mathcal{O}_3 = \mathbf{0}$. Furthermore, since (35) does not hold, one has $\mathbf{d}_{k+3} = \mathbf{d}_{k+2} = \mathbf{d}_{k+1}$. Then, regardless of $\mathbf{d}_k$, $\mathcal{O}_4 = \mathbf{0}$. Therefore, $\mathcal{O}[k,k+4]\mathbf{c} = \mathbf{0}$, which means that for the DT-LTV system (10) to be observable, (35) must hold.

- $\mathbf{d}_{k+1} \neq \mathbf{d}_{k+2}$

Let $\mathbf{c}_1 = \mathbf{d}_k c_3$, $\mathbf{c}_2$ be given by (18) and $c_3 \neq 0$. Suppose that $b = 0$, which means that $\mathbf{d}_k = \mathbf{d}_{k+2} = \mathbf{d}_{k+3}$, or, alternatively, suppose that $c = 0$, which means that $\mathbf{d}_k = \mathbf{d}_{k+1} = \mathbf{d}_{k+3}$. In both situations, it follows from *Theorem* 1 that $\mathcal{O}_1 = \mathcal{O}_2 = \mathcal{O}_3 = \mathbf{0}$. As to $\mathcal{O}_4$, it obeys

$$\mathcal{O}_4 = \begin{cases} \dfrac{b}{a}\dfrac{T_{k+2}}{T_k + T_{k+1}}c_3\mathbf{S}^2(\mathbf{d}_{k+3})\mathbf{d}_{k+1} = \mathbf{0}, & c = 0 \\ \dfrac{c}{a}\dfrac{T_{k+1} + T_{k+2}}{T_k}c_3\mathbf{S}^2(\mathbf{d}_{k+3})\mathbf{d}_{k+2} = \mathbf{0}, & b = 0 \end{cases}.$$

With both b and c different from 0 it is possible to check by long, but straightforward computations that if (35) does not hold, then $\mathcal{O}_4 = \mathbf{0}$, which means (10) is not observable. Therefore, for the DT-LTV system (10) to be observable, (35) must hold.

Regarding the sufficiency of (35) being true in addition to $\mathbf{d}_k$, $\mathbf{d}_{k+1}$, $\mathbf{d}_{k+2}$ being all non-collinear, suppose that both statements hold and that the DT-LTV (10) is not observable, which is equivalent to say that there exists a unit vector $\mathbf{c}$ such that $\mathcal{O}[k,k+4]\mathbf{c} = \mathbf{0}$. Thus, from (14) it must be $\mathbf{c}_1 = \mathbf{d}_k c_3$. Let $c_3 = 0$, implying $\mathbf{c}_1 = \mathbf{0}$. For $\mathcal{O}_2$ to be zero, it must be $\mathbf{c}_2 = \pm\mathbf{d}_{k+1}$. Substituting $\mathbf{c}$ in (16) leads to (22), whose only solution is, under *Assumption* 2, $\mathbf{d}_{k+1} = \mathbf{d}_{k+2}$. Now, given the current $\mathbf{c}$ and $\mathbf{d}_{k+1} = \mathbf{d}_{k+2}$, setting (36) to zero yields $\mathbf{S}^2(\mathbf{d}_{k+3})\mathbf{d}_{k+1} = \mathbf{0}$, whose only solution, under *Assumption* 2, is $\mathbf{d}_{k+1} = \mathbf{d}_{k+3}$, but this means that $\mathbf{d}_{k+1} = \mathbf{d}_{k+2} = \mathbf{d}_{k+3}$, hence (35) cannot hold. Next, let $c_3 \neq 0$ and $\mathbf{c}_2 = \mathbf{0}$. From (15) and (16) one gets $\mathbf{d}_k = \mathbf{d}_{k+1}$ and $\mathbf{d}_{k+1} = \mathbf{d}_{k+2}$, respectively, but this means that having all three directions being non-collinear cannot hold. Thus, let $\mathbf{c}_2 \neq \mathbf{0}$, more specifically decompose it as expressed by (25). Recall the proof of *Theorem* 1: it was shown that, given the current value of $\mathbf{c}$, for $\mathcal{O}_3$ to be zero the original observability condition (12) could not hold when assuming $\mathbf{d}_{k+1} \neq \mathbf{d}_{k+2}$. However, having $\mathbf{d}_{k+1} = \mathbf{d}_{k+2}$ does not prevent collinearity with $\mathbf{d}_k$ from being verified. Still, the only solution for $\mathcal{O}_3 = \mathbf{0}$ is $\mathbf{d}_k = \mathbf{d}_{k+2}$, but in this case the three consecutive directions

This article has been accepted for publication in a future issue of this journal, but has not been fully edited. Content may change prior to final publication. Citation information: DOI 10.1109/TAES.2018.2831118, IEEE Transactions on Aerospace and Electronic Systems

are all collinear. On the other hand, when $\mathbf{d}_{k+1} \neq \mathbf{d}_{k+2}$, and further supposing that (12) does not hold, one has $\boldsymbol{\mathcal{O}}_3 = \mathbf{0}$ for $\mathbf{c}_1 = \mathbf{d}_k c_3$, and $\mathbf{c}_2$ and β as given by (25) and (28), respectively. Finally, make the appropriate substitutions in (36) and simplify in order to obtain

$$\begin{aligned}&\boldsymbol{\mathcal{O}}_4 \frac{1-\left(\mathbf{d}_{k+2}^T \mathbf{d}_{k+1}\right)^2}{c_3} \frac{T_k}{T_{k+1}} = \\ &-\left(\mathbf{I}-\frac{T_{k+2}}{T_k+T_{k+1}} \mathbf{S}^2(\mathbf{d}_{k+3})\right) \mathbf{d}_{k+1} \mathbf{d}_{k+1}^T \mathbf{S}^2(\mathbf{d}_{k+2}) \mathbf{d}_k \\ &+\left(1-\left(\mathbf{d}_{k+2}^T \mathbf{d}_{k+1}\right)^2\right)\left[\frac{T_{k+2}}{T_{k+1}} \mathbf{S}^2(\mathbf{d}_{k+3})-\mathbf{I}\right] \mathbf{d}_k \\ &-\mathbf{d}_{k+3}\left(\mathbf{d}_{k+3}^T \mathbf{d}_{k+2}\right) \mathbf{d}_{k+2}^T \mathbf{S}^2(\mathbf{d}_{k+1}) \mathbf{d}_k .\end{aligned}$$

According to (34), this previous result can be rewritten in a simpler format as

$$\boldsymbol{\mathcal{O}}_4 = -c_3 \mathbf{S}^2(\mathbf{d}_{k+3}) \left[\frac{b}{a} \frac{T_{k+2} \mathbf{d}_{k+1}}{T_k + T_{k+1}} + \frac{c}{a} \frac{T_{k+1} + T_{k+2}}{T_k} \mathbf{d}_{k+2}\right].$$

Due to *Assumption* 2 (two directions cannot oppose each other) and to the fact that $\mathbf{d}_{k+1} \neq \mathbf{d}_{k+2}$, the term

$$\frac{b}{a} \mathbf{d}_{k+1} \frac{T_{k+2}}{T_k + T_{k+1}} + \frac{c}{a} \mathbf{d}_{k+2} \frac{T_{k+1} + T_{k+2}}{T_k} \tag{37}$$

cannot be null, which means that for $\boldsymbol{\mathcal{O}}_4$ to be zero, then (37) must be aligned with $\mathbf{d}_{k+3}$, i.e.

$$\mathbf{d}_{k+3} = \frac{b}{ad} \frac{T_{k+2}}{T_k + T_{k+1}} \mathbf{d}_{k+1} + \frac{c}{ad} \frac{T_{k+1} + T_{k+2}}{T_k} \mathbf{d}_{k+2},$$

where d is the normalizing constant that ensures $\|\mathbf{d}_{k+3}\| = 1$. Hence, the relaxed condition (35) cannot hold. Thus, it has been shown that if a unit vector $\mathbf{c}$ exists, with $c_3 \neq 0$, such that $\boldsymbol{\mathcal{O}}[k, k+4]\mathbf{c} = \mathbf{0}$, then (35) cannot hold. But that had already been shown for $c_3 = 0$, which allows to conclude that if a unit vector $\mathbf{c}$ exists such that $\boldsymbol{\mathcal{O}}[k, k+4]\mathbf{c} = \mathbf{0}$ or, equivalently, if the DT-LTV system (10) is not observable, then (35) cannot be true. Therefore, by contraposition, if (35) holds, the DT-LTV system (10) is observable, thus concluding the proof of sufficiency. □

Remark 1. *The previous theorem studied the observability of the DT-LTV system* (10) *when four consecutive and coplanar direction vectors are considered. Conversely, in the absence of coplanarity among these vectors, one simply resorts to* Theorem *1. Unfortunately, as opposed to* Theorem *1, the observability condition stated in* Theorem *3 lacks an intuitive geometric interpretation.*

C. Kalman Filter

Section III-A introduced a DT-LTV system for source localization based on direction and velocity measurements. Its observability was then studied in Section III-B. Regarding linear estimators, the Kalman filter follows as the natural estimation solution and, because it is widely known, its design is omitted in this paper.

Regarding the Kalman filter model, its system dynamics, including additive system disturbances and sensor noise, can be written as

$$\begin{cases}\hat{\mathbf{x}}_{k+1} = \mathbf{A}_k \hat{\mathbf{x}}_k + \mathbf{n}_k \\ \hat{\mathbf{y}}_{k+1} = \mathbf{C}_{k+1} \hat{\mathbf{x}}_{k+1} + \mathbf{w}_{k+1}\end{cases},$$

where $\mathbf{n}_k \in \mathbb{R}^7$ is zero-mean white Gaussian noise, with $E[\mathbf{n}_k \mathbf{n}_j^T] = \mathbf{Q}_k \delta_{k-j}$, $\mathbf{Q}_k \in \mathbb{R}^{7\times 7}$ being the positive semi-definite covariance of the process noise, and where $\mathbf{w}_k \in \mathbb{R}^3$ is also zero-mean white Gaussian noise, with $E[\mathbf{w}_k \mathbf{w}_j^T] = \mathbf{R}_k \delta_{k-j}$, $\mathbf{R}_k \succ \mathbf{0}$, $\mathbf{R}_k \in \mathbb{R}^{3\times 3}$ being the covariance of the observation noise. The noises are assumed to be uncorrelated, whereby $E[\mathbf{n}_k \mathbf{w}_j^T] = \mathbf{0}$, for all k and j, and they are also assumed to be additive, despite the fact that it might not correspond to reality. Thus, the proposed solution is regarded as sub-optimal.

In order to ensure stability of the Kalman filter, stronger forms of observability are required as this is a time-varying system, in particular, uniform complete observability. As such, a new condition is derived, closely related to the one established in (12), but considering uniform bounds in time. Consequently, as this new derivation takes boundedness into account, *Assumption* 2 alone is not enough to support it, which motivates the following updated (but still mild) assumption.

Assumption 3. *Let there be positive constants τ_1, τ_2, δ_1, δ_2 such that, for all $k \geq k_0$,*

$$\delta_1 < \mathbf{d}_k^T \mathbf{d}_{k+1} < 1 - \delta_2, \text{ and } \tau_1 < T_k < \tau_2.$$

The following theorem introduces a sufficient condition that, if verified, deems the DT-LTV system (10) uniformly completely observable (u.c.o.), thus guaranteeing that the Kalman filter presents GES error dynamics.

Theorem 4. *Given an integer N, consider any three consecutive direction measurements in the interval $\mathcal{I} := [k, k+N]$, given by $\{\mathbf{d}_{k+l}, \mathbf{d}_{k+l+1}, \mathbf{d}_{k+l+2}\}$, with $0 \leq l \leq N-2$. Then, the DT-LTV system* (10) *is u.c.o. if*

$$\exists_{\sigma>0}\ \forall_{k\geq k_0} \quad f_{Obs} \geq \sigma, \tag{38}$$

where,

$$\begin{aligned}f_{Obs} :=\ & 1 + 2\mathbf{d}_{k+l}^T \mathbf{d}_{k+l+1} \mathbf{d}_{k+l}^T \mathbf{d}_{k+l+2} \mathbf{d}_{k+l+1}^T \mathbf{d}_{k+l+2} \\ & - \left(\mathbf{d}_{k+l}^T \mathbf{d}_{k+l+2}\right)^2 - \left(\mathbf{d}_{k+l}^T \mathbf{d}_{k+l+1}\right)^2 - \left(\mathbf{d}_{k+l+1}^T \mathbf{d}_{k+l+2}\right)^2 .\end{aligned}$$

Proof. According to [27, Definition 7.153], the DT-LTV system (10) is u.c.o. if

$$\exists_{\substack{N>0\\ \alpha>0\\ \beta>0}}\ \forall_{k\geq k_0} \quad \alpha \mathbf{I} \leq \boldsymbol{\mathcal{J}}[k+N, k] \leq \beta \mathbf{I}, \tag{39}$$

with

$$\boldsymbol{\mathcal{J}}[k+N, k] = \sum_{i=k}^{k+N} \mathbf{\Phi}^T[i, k+N] \mathbf{C}_i^T \mathbf{C}_i \mathbf{\Phi}[i, k+N],$$

where, for $i \in [k, k+N]$, the transition matrix $\mathbf{\Phi} \in \mathbb{R}^{7\times 7}$, associated with the dynamics matrix $\mathbf{A}_k$, is given by

$$\mathbf{\Phi}[k+N, i] = \begin{cases}\prod_{l=1}^{k+N-i} \mathbf{A}_{k+N-l}, & i < k+N \\ \mathbf{I}, & i = k+N\end{cases}. \tag{40}$$

Regarding (40), it is a simple matter of computations to show that from (11) one can write, for $i < k+N$,

$$\prod_{l=1}^{k+N-i} \mathbf{A}_{k+N-l} = \begin{bmatrix} \mathbf{I} & \Phi_{12}[i]\mathbf{I} & \mathbf{0} \\ \mathbf{0} & \mathbf{I} & \mathbf{0} \\ \mathbf{0} & \mathbf{\Phi}_{32}[i] & \Phi_{33}[i] \end{bmatrix},$$

with

$$\Phi_{12}[i] := \sum_{l=i}^{k+N-1} T_l, \tag{41}$$

$$\mathbf{\Phi}_{32}[i] := \mathbf{d}_{k+N}^T \sum_{l=i}^{k+N-1} \left\{ T_l \prod_{\substack{m=1 \\ l \leq k+N-2}}^{k+N-1-l} \mathbf{d}_{k+N-m}\mathbf{d}_{k+N-m}^T \right\}, \tag{42}$$

and, finally,

$$\Phi_{33}[i] := \prod_{l=1}^{k+N-i} \mathbf{d}_{k+N-l+1}^T \mathbf{d}_{k+N-l}. \tag{43}$$

Furthermore, under *Assumption* 2, and since $\mathbf{A}_k$ is invertible for every k, notice that

$$\mathbf{\Phi}[i, k+N] = \mathbf{\Phi}^{-1}[k+N, i],$$

which means, according to (41), (42) and (43), that it is possible to write

$$\prod_{l=1}^{k+N-i} \mathbf{A}_{k+N-l}^{-1} = \begin{bmatrix} \mathbf{I} & -\Phi_{12}[i]\mathbf{I} & \mathbf{0} \\ \mathbf{0} & \mathbf{I} & \mathbf{0} \\ \mathbf{0} & -\frac{\mathbf{\Phi}_{32}[i]}{\Phi_{33}[i]} & \frac{1}{\Phi_{33}[i]} \end{bmatrix}.$$

Now, let there be a unit vector $\mathbf{u} = [\mathbf{u}_1^T \; \mathbf{u}_2^T \; u_3]^T \in \mathbb{R}^7$, with $\mathbf{u}_1$,$\mathbf{u}_2 \in \mathbb{R}^3$ and $u_3 \in \mathbb{R}$, such that, for all $\|\mathbf{u}\| = 1$, (39) can be rewritten as

$$\alpha \leq \mathbf{u}^T \boldsymbol{\mathcal{J}}[k+N, k]\mathbf{u} = \sum_{i=k}^{k+N} \|\mathbf{C}_i \mathbf{\Phi}[i, k+N]\mathbf{u}\|^2 \leq \beta. \tag{44}$$

The right inequality in (44) is easily shown to be always true since all matrices involved are norm-bounded and well defined by construction. Regarding the left inequality in (44), start by expanding the summation as follows

$$\begin{aligned} \alpha \leq & \|\mathbf{C}_k \mathbf{\Phi}[k, k+N]\mathbf{u}\|^2 + \ldots + \|\mathbf{C}_{k+l} \mathbf{\Phi}[k+l, k+N]\mathbf{u}\|^2 \\ & + \|\mathbf{C}_{k+l+1} \mathbf{\Phi}[k+l+1, k+N]\mathbf{u}\|^2 \\ & \quad + \|\mathbf{C}_{k+l+2} \mathbf{\Phi}[k+l+2, k+N]\mathbf{u}\|^2 + \ldots + \|\mathbf{C}_{k+N}\mathbf{u}\|^2. \end{aligned}$$

Notice that, since all terms in the summation are nonnegative, it suffices to show that the sum of three terms verifies the left inequality, for instance, the ones that correspond to the three consecutive directions mentioned above. Hence, the objective is to show

$$\begin{aligned} \alpha \leq & \|\mathbf{C}_{k+l} \mathbf{\Phi}[k+l, k+N]\mathbf{u}\|^2 \\ & + \|\mathbf{C}_{k+l+1} \mathbf{\Phi}[k+l+1, k+N]\mathbf{u}\|^2 \\ & + \|\mathbf{C}_{k+l+2} \mathbf{\Phi}[k+l+2, k+N]\mathbf{u}\|^2, \end{aligned}$$

which, in view of the composition property of the transition matrix, can be rewritten as

$$\begin{aligned} \alpha \leq & \|\mathbf{C}_{k+l} \mathbf{\Phi}[k+l, k+l+2]\mathbf{\Phi}[k+l+2, k+N]\mathbf{u}\|^2 \\ & + \|\mathbf{C}_{k+l+1} \mathbf{\Phi}[k+l+1, k+l+2]\mathbf{\Phi}[k+l+2, k+N]\mathbf{u}\|^2 \\ & \quad + \|\mathbf{C}_{k+l+2} \mathbf{\Phi}[k+l+2, k+N]\mathbf{u}\|^2. \end{aligned} \tag{45}$$

For the sake of simplicity and readability, let

$$\mathbf{c} := \frac{\mathbf{\Phi}[k+l+2, k+N]\mathbf{u}}{\|\mathbf{\Phi}[k+l+2, k+N]\mathbf{u}\|},$$

such that $\mathbf{c} = [\mathbf{c}_1^T \; \mathbf{c}_2^T \; c_3]^T \in \mathbb{R}^7$ is a unit vector, with $\mathbf{c}_1$,$\mathbf{c}_2 \in \mathbb{R}^3$ and $c_3 \in \mathbb{R}$, and define henceforward $\mathbf{d}_1 := \mathbf{d}_{k+l}$, $\mathbf{d}_2 := \mathbf{d}_{k+l+1}$, and $\mathbf{d}_3 := \mathbf{d}_{k+l+2}$. Notice that $\mathbf{c}$ is well defined as the transition matrix is always invertible. Likewise, let $T_1 := T_{k+l}$ and $T_2 := T_{k+l+1}$. Accordingly, (45) results in

$$\bar{\alpha} \leq J_1 + J_2 + J_3,$$

where

$$\bar{\alpha} = \frac{\alpha}{\|\mathbf{\Phi}[k+l+2, k+N]\mathbf{u}\|^2},$$

$$J_1 = \|\mathbf{c}_1 - \mathbf{d}_3 c_3\|^2,$$

$$J_2 = \left\| \mathbf{c}_1 - \frac{\mathbf{d}_2 c_3}{\mathbf{d}_3^T \mathbf{d}_2} - T_1 \left(\mathbf{I} - \frac{\mathbf{d}_2 \mathbf{d}_3^T}{\mathbf{d}_3^T \mathbf{d}_2} \right) \mathbf{c}_2 \right\|^2,$$

and

$$\begin{aligned} J_3 = & \left\| \mathbf{c}_1 - \frac{\mathbf{d}_1}{\mathbf{d}_3^T \mathbf{d}_2 \mathbf{d}_2^T \mathbf{d}_1} c_3 \right. \\ & \left. - \left[(T_1 + T_2)\mathbf{I} - \frac{\mathbf{d}_1 \mathbf{d}_3^T \left(T_2 \mathbf{I} + T_1 \mathbf{d}_2 \mathbf{d}_2^T \right)}{\mathbf{d}_3^T \mathbf{d}_2 \mathbf{d}_2^T \mathbf{d}_1} \right] \mathbf{c}_2 \right\|^2. \end{aligned}$$

Resorting to a proof by contraposition, start by assuming that the DT-LTV system (10) is not u.c.o.. In other words, based on (39) and *Assumption* 3, if it is true that

$$\forall_{\bar{\alpha}>0} \; \exists_{\substack{k \geq k_0 \\ \|\mathbf{c}\|=1}} \quad J_1 + J_2 + J_3 < \bar{\alpha},$$

then the condition (38) cannot be verified. From here onwards, as the proof of sufficiency follows similar steps to *Theorem* 1, but considering uniformity bounds, the remainder of the proof is omitted. □

IV. SIMULATION RESULTS

A numerical simulation is presented and discussed in this section to evaluate the achievable performance with the proposed solution for source localization with velocity bias estimation based on direction and velocity measurements. Section IV-A contains a description of the setup considered in the simulations. The Bayesian Cramér-Rao lower bound, computed to evaluate the performance of the proposed solution, is briefly described in Section IV-B. The tuning of the Kalman filter parameters for the proposed solution is addressed in Section IV-C. Finally, in Section IV-D Monte Carlo results are discussed.

A. Setup

Consider an AUV, moving in the presence of ocean currents, that periodically emits an acoustic signal, which can be sampled, for instance, by a receiver equipped with an USBL acoustic positioning system placed at the origin of the inertial reference frame. The initial position of the vehicle is set to $\mathbf{s}_{k=k_0} = [-100 \; -50 \; 0]^T$ m, while the ocean current velocity is set to $\mathbf{b} = [1.2 \; -0.5 \; 0.1]^T$ m/s, both expressed in inertial

This article has been accepted for publication in a future issue of this journal, but has not been fully edited. Content may change prior to final publication. Citation information: DOI 10.1109/TAES.2018.2831118, IEEE Transactions on Aerospace and Electronic Systems

coordinates. The vehicle describes a trajectory as shown in Fig. 1, where one can notice its rich behaviour, in particular it is possible to perceive that the direction of the source with respect to the origin of the frame is always changing, hence ensuring that, according to **Theorem 3**, observability is attained. Furthermore, uniform complete observability is also attained, as confirmed through a numerical inspection of the dataset.

It is worth noticing that **Theorem 3** alone provides a clear insight as to what kind of trajectory one should avoid, more specifically all trajectories where the source moves towards the origin of the frame along the same direction. However, there are simple trajectories that, despite verifying the observability conditions of the problem, dramatically reduce the performance of the proposed solution, for instance, any straight line that does not pass through the origin. In this case, the direction indeed keeps changing, but its almost indiscernible rate of change, in addition to constant bias and velocity, undermines any chances of good performance. What's more, straight lines are often related to increasingly longer distances, which, when accounting for multiplicative noise in directions, correspond to larger position deviations, thus preventing the filter from converging.

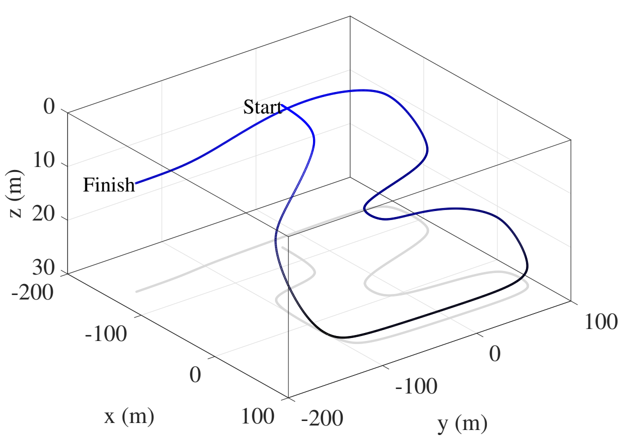

Figure 1: Trajectory described by the source.

A constant sampling period of $T = 1$ s was employed for the direction and velocity measurements. The direction measurements were rotated about random vectors of an angle that follows a zero-mean white Gaussian noise distribution, with standard deviation of $1°$. In turn, the velocity measurements are assumed to be corrupted by additive zero-mean white Gaussian noise, with standard deviation of 0.01 m/s. Upon sampling, direction measurements are assigned to the output $\mathbf{y}_k$ of the DT-LTV system (10) in the form of (9), whereas velocity measurements are assigned to the input $\mathbf{u}_k$.

B. Bayesian Cramér-Rao Lower Bound

The Kalman filter introduced in Section III-C for the DT-LTV system (10) is sub-optimal in the sense that noise sequences considered herein may not be additive in reality. Moreover, since the final linear filter design stems from the original nonlinear discrete-time system (4), a comparison in terms of performance between the proposed solution and an estimator for (4) is appropriate. For instance, in spite of not guaranteeing stability, the EKF is one of the most widely used tools to approach the design of estimators for nonlinear systems, which still poses multiple challenges. However, in a few cases, there exist theoretical bounds on achievable performance. Recall the discrete-time system introduced in (4) that features a linear process and nonlinear output. For this particular system, while considering additive white Gaussian noise, the BCRLB can be computed. The result provides, for any given causal (realizable) unbiased estimator, a lower bound on its covariance matrix [28].

Consider the general discrete-time system

$$\begin{cases} \mathbf{x}_{k+1} = \mathbf{F}_k \mathbf{x}_k + \mathbf{B}_k \mathbf{u}_k + \mathbf{n}_k \\ \mathbf{y}_k = \mathbf{h}(\mathbf{x}_k) + \mathbf{w}_k \end{cases}, \tag{46}$$

where $\mathbf{x}_k$ is the state vector; $\mathbf{u}_k$ is a deterministic system input; $\mathbf{y}_k$ is the system output, expressed nonlinearly in function of the state vector through $\mathbf{h}(\mathbf{x}_k)$; $\mathbf{n}_k$ corresponds to a zero mean multivariate normal distribution with covariance $\mathbf{Q}_k$; and $\mathbf{w}_k$ corresponds to a zero mean multivariate normal distribution with covariance $\mathbf{R}_k$. The implementation of the EKF resorts to a recursion which can be achieved in a almost identical way for the case of the BCRLB, except that the Jacobian of $\mathbf{h}(\mathbf{x}_{k+1})$ is evaluated at the true state (see [28, Section 2.3.3]). The BCRLB $\boldsymbol{\mathcal{B}}_k$ obeys

$$\boldsymbol{\mathcal{B}}_k = \mathbf{J}_k^{-1},$$

where $\mathbf{J}_k$ satisfies the recursion

$$\mathbf{J}_{k+1} = \left(\mathbf{Q}_k + \mathbf{F}_k \mathbf{J}_k^{-1} \mathbf{F}_k^T\right)^{-1} + \mathbf{P}_{k+1}.$$

The covariance reduction due to the measurements is denoted by $\mathbf{P}_{k+1}$, which corresponds to an expected value determined as

$$\mathbf{P}_{k+1} = E_{\mathbf{x}_{k+1}} \left\{ \tilde{\mathbf{H}}^T(\mathbf{x}_{k+1}) \mathbf{R}_{k+1}^{-1} \tilde{\mathbf{H}}(\mathbf{x}_{k+1}) \right\}, \tag{47}$$

where $\tilde{\mathbf{H}}(\mathbf{x}_{k+1})$ is the Jacobian of the nonlinear observation function evaluated at $\mathbf{x}_{k+1}$.

The computation of the expected value presented in (47) is made according to $\mathbf{x}_{k+1}$. In view of this circumstance, Monte Carlo simulations are often used in evaluating the computation. However, when designing estimators for nonlinear systems, evaluating the achievable performance along specific or nominal trajectories $\bar{\mathbf{x}}_k$ can be of interest. Since this paper addresses that procedure, a simplified version of $\mathbf{P}_{k+1}$ can be written as

$$\mathbf{P}_{k+1} = \tilde{\mathbf{H}}^T(\bar{\mathbf{x}}_{k+1}) \mathbf{R}_{k+1}^{-1} \tilde{\mathbf{H}}\left(\bar{\mathbf{x}}_{k+1}\right).$$

As explained in [28], the EKF differs from the BCRLB only in terms of Jacobians. Regarding the lower bound, the Jacobians disregard the estimated trajectories and are instead computed at the nominal trajectories $\bar{\mathbf{x}}_k$. Considering additive noise in the velocity measurements collected from the source, and further considering that the direction measurements are rotated about random vectors of an angle that follows a zero-mean white Gaussian noise distribution, with standard deviation of $1°$, the discrete-time nonlinear system (4) can be written in the form of (46). Hence, $\boldsymbol{\mathcal{B}}_k$ can be computed, and it is shown in the sequel.

This article has been accepted for publication in a future issue of this journal, but has not been fully edited. Content may change prior to final publication. Citation information: DOI 10.1109/TAES.2018.2831118, IEEE Transactions on Aerospace and Electronic Systems

C. Kalman Filter application

Building on the results presented in Section III, a Kalman filter is developed for the DT-LTV system (10), which yields GES error dynamics. Regarding the tuning of the Kalman filter parameters, they were set empirically in an effort to adjust the performance of the proposed solution. Specifically, the process covariance matrix $\mathbf{Q}$ was chosen as $\mathrm{diag}(10^{-3}\mathbf{I}, 10^{-4}\mathbf{I}, 9)$, while the output noise covariance matrix $\mathbf{R}$ was set to $10\mathbf{I}$.

The initial condition of the filter was set to zero for all system states. By doing so, the filter is initialized with large position and range errors, and it practically holds no information whatsoever on the unknown parameter that corresponds to the velocity bias. In turn, the initial covariance of the filter, $\mathbf{P}_{k=k_0}$, was set to $\mathrm{diag}(10^4\mathbf{I}, 10\mathbf{I}, 10^4)$.

Fig. 2 depicts the initial convergence of the position and velocity errors. As seen from both plots, the convergence rate of the filter is moderate for this kind of application, which is in line with the expectations when accounting for the chosen (realistic) sampling time of 1 s. Notwithstanding, the error converges to the neighbourhood of 0. Since sensor noise is involved, the errors do not converge to 0. Fig. 3 depicts the detailed evolutions of the position and velocity errors, where dashed lines are used to illustrate the 1σ bounds obtained from the covariance of the Kalman filter (corresponding to the square root of the diagonal elements of $\mathbf{P}_k$). In solid thicker lines is plotted the 1σ BCRLB (more specifically, the square root of the diagonal elements of $\boldsymbol{\mathcal{B}}_k$). From Fig. 3 one can conclude that the achievable performance attained with the proposed solution is consistent with the BCRLB.

For the sake of completeness, the evolution of the range errors is shown in Fig. 4. As seen from the plot, the rate of convergence for this particular error is quite high, and most noticeably, in steady-state, the error remains below 0.5 m. The 1σ bound obtained from the covariance of the Kalman filter is again depicted in dashed lines, which correspond to the square root of the last diagonal element of matrix $\mathbf{Q}$. Since the range is not explicitly estimated for the nonlinear case, the BCRLB for this state is not applicable.

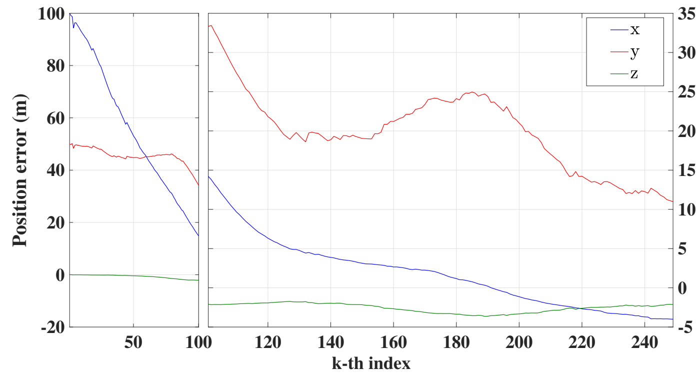

(a) Position error.

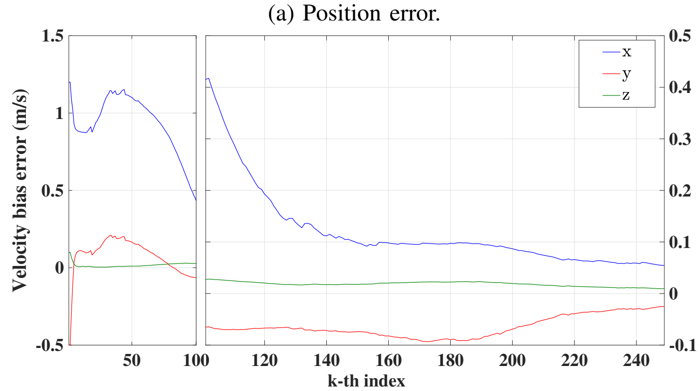

(b) Velocity bias error.

Figure 2: Initial convergence of errors (Kalman Filter).

Table I: Performance comparison in terms of averaged standard deviation.

Variable (Unit)	KF	EKF	BCRLB
$\tilde{\mathbf{s}}_x$ (m)	0.2311	1.8060	0.0727
$\tilde{\mathbf{s}}_y$ (m)	0.1168	2.2499	0.0596
$\tilde{\mathbf{s}}_z$ (m)	0.1210	0.5643	0.0266
$\tilde{\mathbf{b}}_x$ (mm/s)	0.5825	5.6	0.1810
$\tilde{\mathbf{b}}_y$ (mm/s)	0.5371	18.5	0.2434
$\tilde{\mathbf{b}}_z$ (mm/s)	0.3795	4.9	0.1043

D. Performance Comparison

The proposed solution was compared to the performance achieved by an EKF applied to the original nonlinear system (4). Due to the existence of a singularity in the EKF when the source position is zero, the initial condition for the position was set at $\hat{\mathbf{x}}^1_{k=k_0} = [100\ 100\ 0]$ m, while the velocity bias was set to zero. The values of matrices $\mathbf{Q}$, $\mathbf{R}$ and $\mathbf{P}_{k=k_0}$ were set in an effort to deem the comparison with the proposed solution as fair as possible.

The initial convergence of the position and velocity bias errors are depicted in Fig. 5. Compared to the proposed solution, given the same initial conditions, the rate of convergence of the EKF is much slower, and it shows much larger initial transients. Fig. 6 depicts the detailed evolution of the position and velocity errors, along with the 1σ bounds computed from the EKF covariance matrix $\mathbf{P}_k$ and from the lower bound $\boldsymbol{\mathcal{B}}_k$. In steady-state, the performance of the EKF resembles that of the proposed solution, although presenting slightly larger deviations. Nevertheless, the EKF does not offer guarantees of global convergence.

Finally, to better assess the differences in the performance between the proposed solution and the EKF, the Monte Carlo method was applied. The simulation was carried out 1000 times with different, randomly generated noise signals. Considering significant statistical data extracted in steady state (for $k \geq 500$), the standard deviations of the errors were computed for each simulation and averaged over the set of simulations. Table I depicts the results obtained from both the proposed solution and from the EKF. In addition, the 1σ lower bound $\boldsymbol{\mathcal{B}}_k$ was computed in steady state and averaged over the 1000 simulations. The result is shown in the table as well.

In terms of averaged steady-state performance, the EKF exhibits larger standard deviations for all errors, while the proposed solution achieves a performance that behaves closer to that of the BCRLB.

This article has been accepted for publication in a future issue of this journal, but has not been fully edited. Content may change prior to final publication. Citation information: DOI 10.1109/TAES.2018.2831118, IEEE Transactions on Aerospace and Electronic Systems

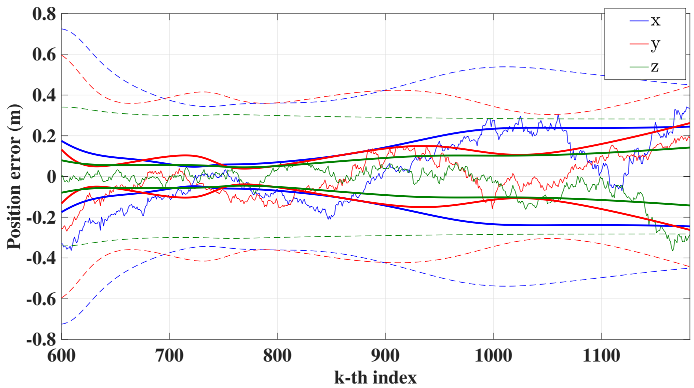

(a) Position error.

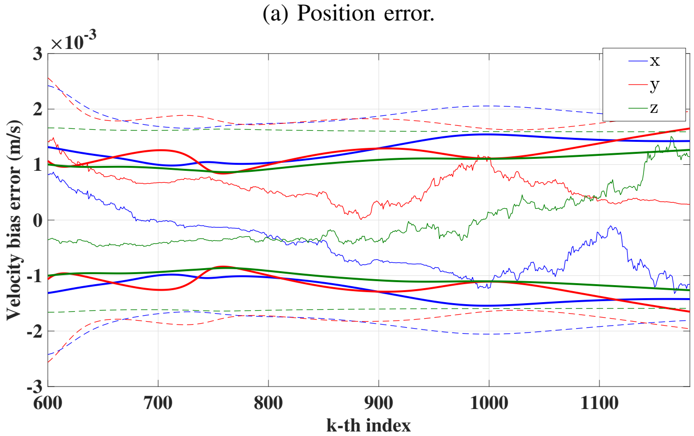

(b) Velocity bias error.

Figure 3: Steady-state evolution of errors (Kalman Filter).
Dashed Lines - $\pm\sqrt{\mathbf{P}_k(i,i)}$.
Solid Lines - $\mathbf{x}_k(i) - \hat{\mathbf{x}}_k(i)$.
Solid Thick Lines - $\pm\sqrt{\boldsymbol{\mathcal{B}}_k(i,i)}$.
$i = 1, 2, 3$ for Position; $i = 4, 5, 6$ for Velocity Bias.

V. EXPERIMENTAL RESULTS

This section presents and discusses experimental results that allow to assess the achievable performance of the proposed filtering technique in a real world application.

The design of trajectories must take into account Assumptions 1 and 2 in particular; the claims of both Theorems 1 and 3; and, the fact that the characteristics of the real noise differ from the ones assumed in the paper. In summary, under these conditions, a trajectory spanning a confined three-dimensional space and featuring time-varying velocities should yield a good estimation performance.

Briefly, while in pursuit of a typical underwater mission scenario, a set of trials was carried out in a shallow enclosed lake wherein a surface vehicle equipped with a submerged acoustic transponder described a trajectory as depicted in Fig. 7.

The surface vehicle was equipped with a GPS antenna in order to obtain ground-truth position and velocity measurements. In turn, direction measurements were taken with respect to a fixed USBL acoustic receiver, whose position was regarded as the origin of the inertial reference frame. This receiver consists of an integrated ultra-short baseline acoustic positioning system aided by an inertial navigation system. It

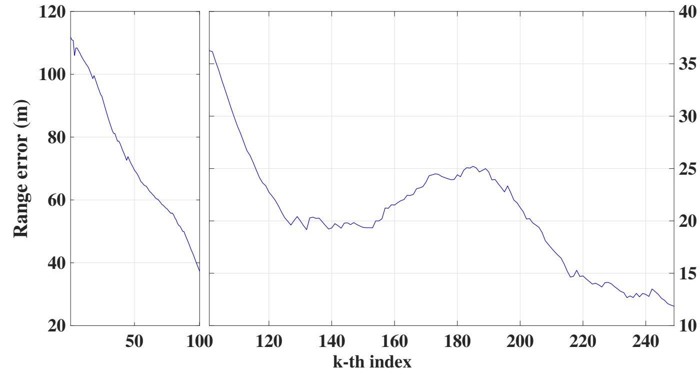

(a) Initial convergence.

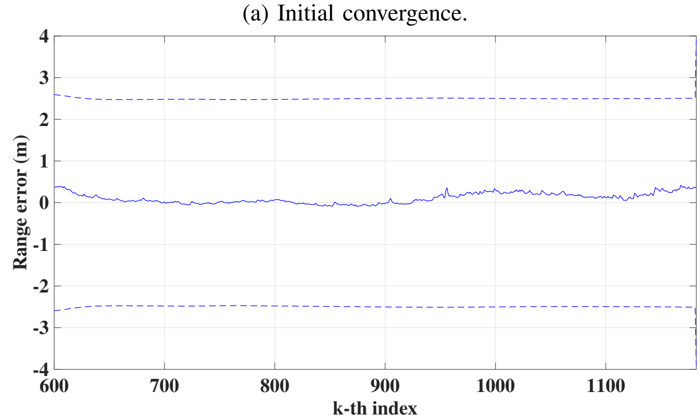

(b) Steady-state evolution.

Figure 4: Evolution of range errors (Kalman Filter).

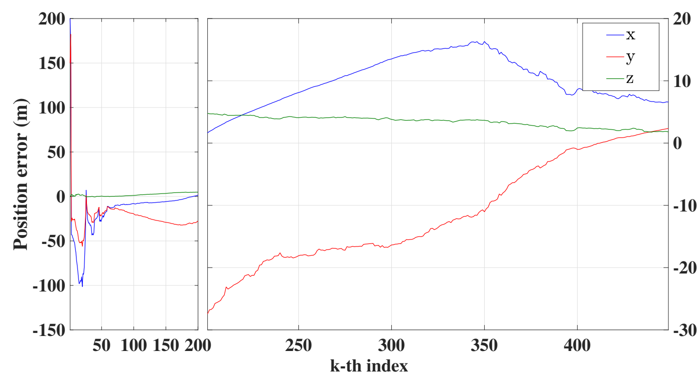

(a) Position error.

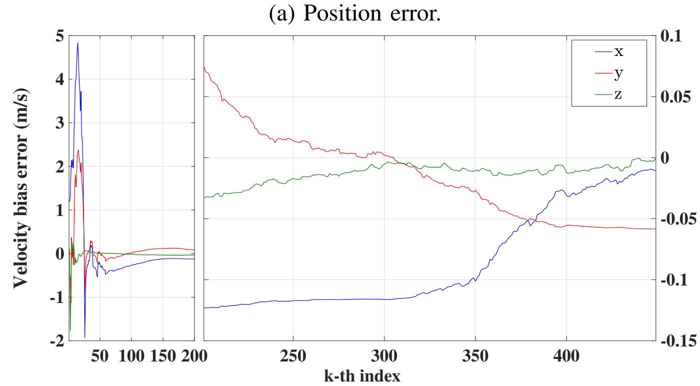

(b) Velocity bias error.

Figure 5: Initial convergence of Extended Kalman Filter errors.

This article has been accepted for publication in a future issue of this journal, but has not been fully edited. Content may change prior to final publication. Citation information: DOI 10.1109/TAES.2018.2831118, IEEE Transactions on Aerospace and Electronic Systems

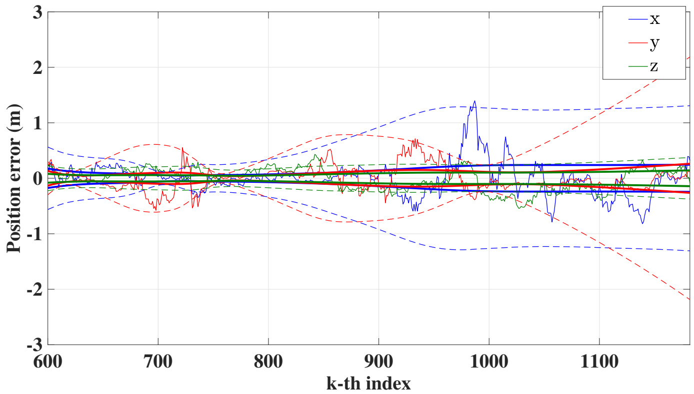

(a) Position error.

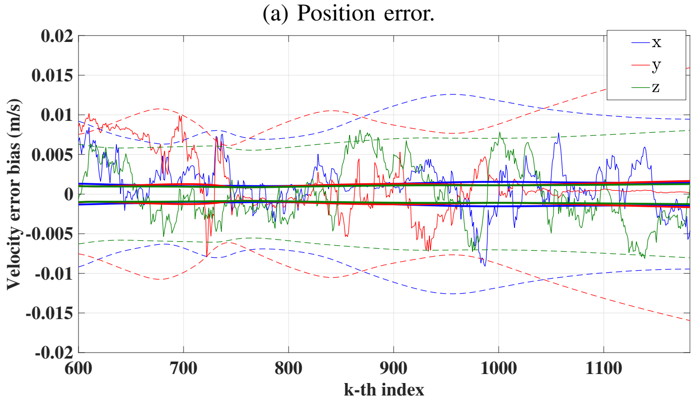

(b) Velocity bias error.

Figure 6: Steady-state evolution of Extended Kalman Filter errors.
Dashed Lines - $\pm\sqrt{\mathbf{P}_k(i,i)}$.
Solid Lines - $\mathbf{x}_k(i) - \hat{\mathbf{x}}_k(i)$.
Solid Thick Lines - $\pm\sqrt{\boldsymbol{\mathcal{B}}_k(i,i)}$.
$i = 1, 2, 3$ for Position; $i = 4, 5, 6$ for Velocity Bias.

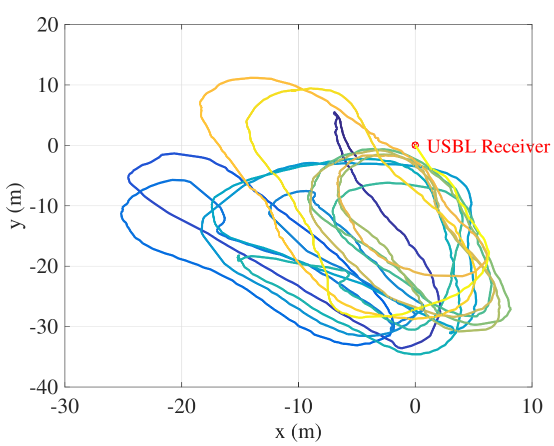

Figure 7: Trajectory described by the source. Color gradient indicates evolution in time: light yellow - start; dark blue - end.

features an array comprising four hydrophones assembled in a non-planar configuration in addition to an acoustic projector that emits a known signal periodically, as seen in Fig. 8. The reader is referred to [29] for further details about the design and development of this underwater localization device.

Figure 8: USBL Receiver.

We remark that the purpose of this experiment is to assess *a posteriori* the performance of the proposed linear time-varying estimator in the presence of real data, more specifically direction measurements based on acoustic signal propagation and GPS velocities. Notwithstanding, given the properties of the lake and the fact that both the receiver and the transponder were at the same depth, the linear estimator was applied considering a two-dimensional framework. In addition to the previous considerations, a constant bias ($\mathbf{b} = [0.33\ 0.66]^T$) was added over the GPS velocity readings to emulate water currents, which were absent in the lake. The sampling times associated with the measurements are shown in Fig. 9.

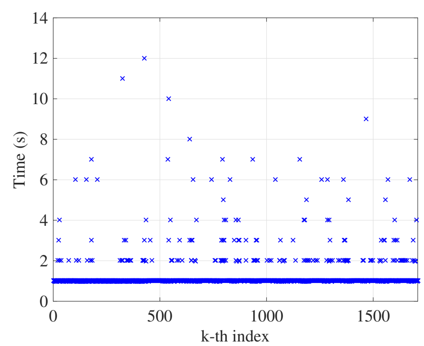

Figure 9: Sampling times during the experiment.

The variation of the sampling time is fairly evident, with a few occurrences above 5 s, which influences the performance of the filter in light of *Assumption* 1. The non-constant sampling time is primarily a result of the distance between the emitter and the receiver changing over time. On top of that, the lake properties induce sampling loss. Shallow waters and bottom shoals are responsible for an increase in the number of invalid measurements by causing strong multi-path reflections which, due to their nature, are rejected by an on-line outlier removal tool.

The initial condition for the position was set at $\hat{\mathbf{x}}^1_{k=k_0} = [100\ \ 100]^T$ m, while states corresponding to the velocity bias and the range were set to zero. To tune the Kalman filter, the state disturbance covariance matrix $\mathbf{Q}$ was chosen as $\text{diag}(10^{-2}\mathbf{I}, 10^{-2}\mathbf{I}, 10^{-2})$ and the output noise covariance

This article has been accepted for publication in a future issue of this journal, but has not been fully edited. Content may change prior to final publication. Citation information: DOI 10.1109/TAES.2018.2831118, IEEE Transactions on Aerospace and Electronic Systems

matrix $\mathbf{R}$ was set to $10\mathbf{I}$. The initial convergence of the position and velocity errors is depicted in Fig. 10, while the detailed evolutions of the position and velocity errors are depicted in Fig. 11, along with the 1σ bounds obtained from the covariance matrix $\mathbf{P}$, represented in dashed lines. For the sake of completeness, the evolution of the range errors is shown in Fig. 12. Overall, the filter presents a good rate of convergence for both the position and velocity bias errors. Most noticeably is that the position and velocity bias errors remain, most of the time, below 2 m and 0.01 m/s, respectively, which are quite good results considering the harsh conditions imposed by the environment, specially when accounting for large sampling rates, which strongly influence the quality of the estimation. These large sampling rates are also responsible for the spikes observed in the plots, which stem from the filter holding to the same estimate for a long period of time.

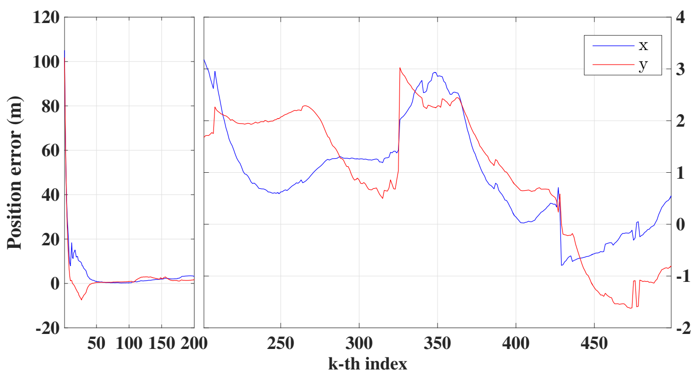

(a) Position error.

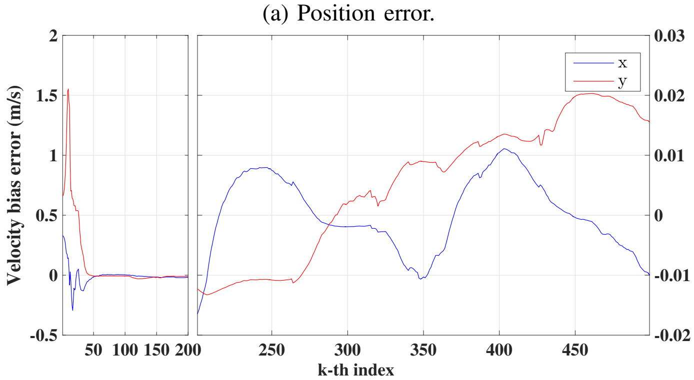

(b) Velocity bias error.

Figure 10: Convergence of errors.

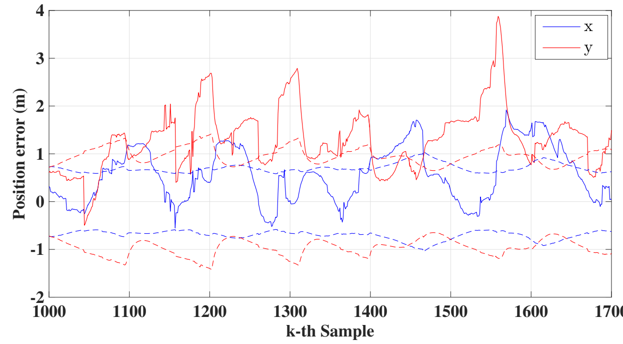

(a) Position error.

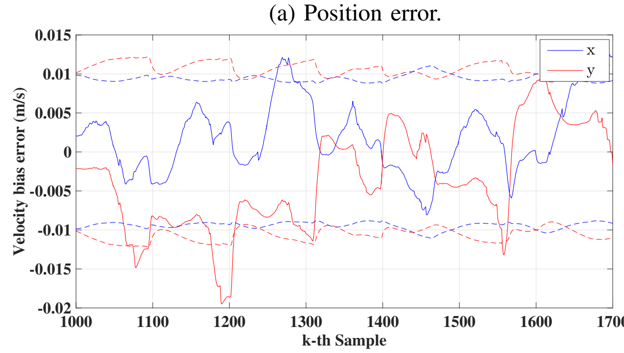

(b) Velocity bias error.

Figure 11: Steady-state evolution of errors.

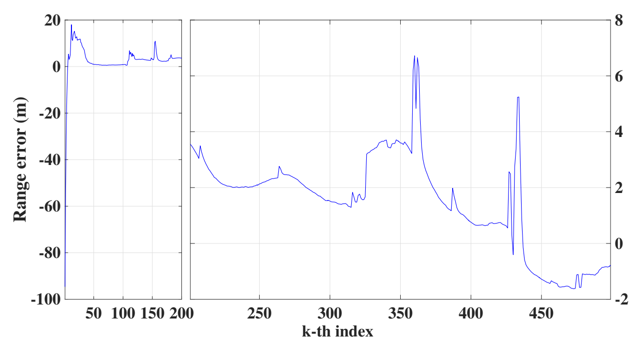

(a) Initial convergence.

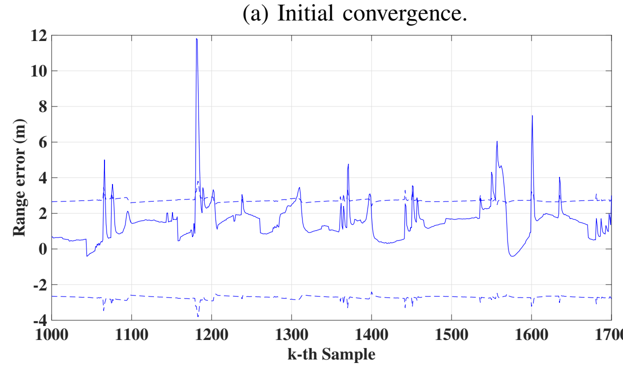

(b) Steady-state evolution.

Figure 12: Evolution of range errors.

VI. CONCLUSIONS

This paper addressed the problem of source localization and velocity bias estimation based on direction and velocity measurements. A discrete-time augmented linear time-varying system was derived whose observability was addressed resorting to a necessary and sufficient condition that is related to the motion of the source. Moreover, based on the boundedness of this same condition, a stronger form of observability was ensured, in particular the system was shown to be uniformly completely observable, hence allowing the design of a linear estimator with GES error dynamics. A Kalman filter was implemented and its performance was thoroughly assessed resorting to realistic simulations considering additive white noise. The proposed solution was then compared to both an EKF and the BCRLB via Monte Carlo runs, exhibiting a performance akin to that of the BCRLB. Finally, a set of experimental results was featured that validates the proposed filtering technique as a viable option for underwater tracking solutions.

REFERENCES

[1] Y. Bar-Shalom, T. Kirubarajan, and X.-R Li. *Estimation with Applications to Tracking and Navigation*. John Wiley & Sons, Inc., New York, NY, USA, 2002.

[2] X.-R. Li and V.P. Jilkov. Survey of maneuvering target tracking. Part I. Dynamic models. *IEEE Transactions on Aerospace and Electronic Systems*, 39(4):1333–1364, Oct 2003.

[3] D.L. Wangsness. A New Method of Position Estimation Using Bearing Measurements. *IEEE Transactions on Aerospace and Electronic Systems*, AES-9(6):959–960, Nov 1973.

[4] D. Mušicki. Bearings only single-sensor target tracking using gaussian mixtures. *Automatica*, 45(9):2088 – 2092, 2009.

[5] V.P. Panakkal and R. Velmurugan. Bearings-only tracking using derived heading. In *Aerospace Conference, 2010 IEEE*, pages 1–11, March 2010.

[6] P. Batista, C. Silvestre, and P. Oliveira. Single range aided navigation and source localization: Observability and filter design. *Systems & Control Letters*, 60(8):665 – 673, 2011.

[7] Y. Cao. UAV circumnavigating an unknown target under a GPS-denied environment with range-only measurements. *Automatica*, 55:150 – 158, 2015.

[8] D.-H. Shin and T.-K. Sung. Comparisons of error characteristics between TOA and TDOA positioning. *IEEE Transactions on Aerospace and Electronic Systems*, 38(1):307–311, Jan 2002.

[9] Y. Wang and K.C. Ho. TDOA Source Localization in the Presence of Synchronization Clock Bias and Sensor Position Errors. *IEEE Transactions on Signal Processing*, 61(18):4532–4544, Sept 2013.

[10] P. Batista. Long baseline navigation with clock offset estimation and discrete-time measurements. *Control Engineering Practice*, 35:43–53, 2015.

[11] Y. Ji, C. Yu, and B.D.O. Anderson. Systematic Bias Correction in Source Localization. *IEEE Transactions on Aerospace and Electronic Systems*, 49(3):1692–1709, July 2013.

[12] A.G. Lingren and K.F. Gong. Position and Velocity Estimation Via Bearing Observations. *IEEE Transactions on Aerospace and Electronic Systems*, AES-14(4):564–577, July 1978.

[13] M. Gavish and A.J. Weiss. Performance analysis of bearing-only target location algorithms. *Aerospace and Electronic Systems, IEEE Transactions on*, 28(3):817–828, July 1992.

[14] J. Snyder. Doppler Velocity Log (DVL) navigation for observation-class ROVs. In *OCEANS 2010 MTS/IEEE SEATTLE*, pages 1–9, Sept 2010.

[15] I. Shames, A.N. Bishop, M. Smith, and B.D.O. Anderson. Doppler Shift Target Localization. *IEEE Transactions on Aerospace and Electronic Systems*, 49(1):266–276, Jan 2013.

[16] X. Sheng and Y.-H. Hu. Maximum likelihood multiple-source localization using acoustic energy measurements with wireless sensor networks. *IEEE Transactions on Signal Processing*, 53(1):44–53, Jan 2005.

[17] S.H. Dandach, B. Fidan, S. Dasgupta, and B.D.O. Anderson. A continuous time linear adaptive source localization algorithm, robust to persistent drift. *Systems & Control Letters*, 58(1):7 – 16, 2009.

[18] J.-P. Le Cadre and S. Laurent-Michel. Optimizing the receiver maneuvers for bearings-only tracking. *Automatica*, 35(4):591 – 606, 1999.

[19] J.P. Helferty and D.R. Mudgett. Optimal observer trajectories for bearings only tracking by minimizing the trace of the Cramér-Rao lower bound. In *Decision and Control, 1993., Proceedings of the 32nd IEEE Conference on*, pages 936–939 vol.1, Dec 1993.

[20] D. Moreno-Salinas, A. Pascoal, and J. Aranda. Optimal Sensor Placement for Acoustic Underwater Target Positioning With Range-Only Measurements. *IEEE Journal of Oceanic Engineering*, PP(99):1–24, 2016.

[21] P. Batista, C. Silvestre, and P. Oliveira. GES source localization and navigation based on discrete-time bearing measurements. In *Decision and Control (CDC), 2013 IEEE 52nd Annual Conference on*, pages 5066–5071, Dec 2013.

[22] P. Batista, C. Silvestre, and P. Oliveira. Globally exponentially stable filters for source localization and navigation aided by direction measurements. *Systems & Control Letters*, 62(11):1065–1072, 2013.

[23] P. Batista, C. Silvestre, and P. Oliveira. Navigation systems based on multiple bearing measurements. *IEEE Transactions on Aerospace and Electronic Systems*, 51(4):2887–2899, Oct 2015.

[24] F. Le Bras, T. Hamel, R.E. Mahony, and C. Samson. Observer design for position and velocity bias estimation from a single direction output. *CoRR*, abs/1503.07680, 2015.

[25] W.J. Rugh. *Linear System Theory (2Nd Ed.)*. Prentice-Hall, Inc., Upper Saddle River, NJ, USA, 1996.

[26] D.C. Woffinden and D.K. Geller. Observability Criteria for Angles-Only Navigation. *IEEE Transactions on Aerospace and Electronic Systems*, 45(3):1194–1208, July 2009.

[27] A.H. Jazwinski. *Stochastic Processes and Filtering Theory*. Mathematics in Science and Engineering. Elsevier Science, 1970.

[28] H.L. Van Trees and K. L. Bell. *Bayesian Bounds for Parameter Estimation and Nonlinear Filtering/Tracking*. Wiley-IEEE Press, 2007.

[29] J. Reis, M. Morgado, P. Batista, P. Oliveira, and C. Silvestre. Design and Experimental Validation of a USBL Underwater Acoustic Positioning System. *Sensors*, 16(9):1491, 2016.

Joel Reis received the M.Sc. degree in Aerospace Engineering, in 2013, from the Instituto Superior Técnico, Lisbon, Portugal. In 2014, he enrolled in the Electrical and Computer Engineering Ph.D. program at the University of Macau, where he is currently doing research at the Faculty of Science and Technology under the supervision of Professor Carlos Silvestre. His research interests include estimation theory based on underwater positioning and localization systems, and design of nonlinear attitude estimation algorithms.

Pedro Batista (M'10) received the Licenciatura degree in Electrical and Computer Engineering in 2005 and the Ph.D. degree in 2010, both from Instituto Superior Técnico (IST), Lisbon, Portugal. From 2004 to 2006, he was a Monitor with the Department of Mathematics, IST. Since 2012 he is with the Department of Electrical and Computer Engineering of IST, he where he is currently Assistant Professor. His research interests include sensor-based navigation and control of autonomous vehicles. Dr. Batista has received the Diploma de Mérito twice during his graduation and his Ph.D. thesis was awarded the Best Robotics Ph.D. Thesis Award by the Portuguese Society of Robotics.

This article has been accepted for publication in a future issue of this journal, but has not been fully edited. Content may change prior to final publication. Citation information: DOI 10.1109/TAES.2018.2831118, IEEE Transactions on Aerospace and Electronic Systems

Carlos Silvestre received the Licenciatura degree in Electrical Engineering from the Instituto Superior Tecnico (IST) of Lisbon, Portugal, in 1987 and the Master degree in Electrical Engineering and the Ph.D. degree in Control Science from the same school in 1991 and 2000, respectively. In 2011 he received the Habilitation in Electrical Engineering and Computers also from IST. Since 2000, he is with the Department of Electrical Engineering of the Instituto Superior Tecnico, where he is currently on leave. Since 2015 he is also with Faculty of Science and Technology of the University of Macau where he currently holds a Professor position with the Department of Electrical and Computers Engineering. His current research interests include linear and nonlinear control theory; hybrid systems; multi-agent control systems; networked control systems; inertial navigation systems and real time architectures for complex autonomous systems with application to unmanned air and underwater vehicles.

Paulo Oliveira (SM IEEE) received the "Licenciatura," M.S., and Ph.D. degrees in Electrical and Computer Engineering, and the Habilitation in Mechanical Engineering from Instituto Superior Tecnico (IST), Lisbon, Portugal, in 1991, 2002, and 2016, respectively. He is an Associate Professor in the Department of Mechanical Engineering of IST and Senior Researcher in the Associated Laboratory for Energy, Transports, and Aeronautics. His research interests are in the area of autonomous robotic vehicles with a focus on the fields of estimation, sensor fusion, navigation, positioning, and mechatronics. He is author or coauthor of more than 65 journal papers and 175 conference communications and participated in more than 30 European and Portuguese research projects, over the last 30 years.